Inorganic Chemistry

Article

pubs.acs.org/IC

Sterically Encumbered Tin and Phosphorus *peri*-Substituted Acenaphthenes

Brian A. Chalmers, Kasun S. Athukorala Arachchige, Joanna K. D. Prentis, Fergus R. Knight, Petr Kilian,* Alexandra M. Z. Slawin, and J. Derek Woollins*

EaStCHEM, School of Chemistry, University of St. Andrews, St. Andrews, Fife, KY16 9ST United Kingdom

Supporting Information

ABSTRACT: A group of sterically encumbered *peri*-substituted acenaphthenes have been prepared, containing tin moieties at the 5,6-positions in **1**−**3** ([Acenap$(SnR_3)_2$], Acenap = acenaphthene-5,6-diyl; R_3 = Ph_3 (**1**), Me_3 (**2**); [$(Acenap)_2(SnMe_2)_2$] (**3**)) and phosphorus functional groups at the proximal *peri*-positions in **4** and **5** ([Acenap(PR_2)-(P^iPr_2)] R_2 = Ph_2 (**4**), Ph(^{i}Pr) (**5**)). Bis(stannane) structures **1**−**3** are dominated by repulsive interactions between the bulky tin groups, leading to *peri*-distances approaching the sum of van der Waals radii. Conversely, the *quasi*-linear C_{Ph}-P···P three-body fragments found in bis(phosphine) **4** suggest the presence of a lp(P)−σ^*(P−C) donor−acceptor 3c-4e type interaction, supported by a notably short intramolecular P···P distance and notably large J_{PP} through-space coupling (180 Hz). Severely strained bis(sulfides) **4-S** and **5-S**, experiencing pronounced in-plane and out-of-plane displacements of the exocyclic *peri*-bonds, have also been isolated following treatment of **4** and **5** with sulfur. The resulting nonbonded intramolecular P···P distances, ∼4.05 Å and ∼12% longer than twice the van der Waals radii of P (3.60 Å), are among the largest ever reported *peri*-separations, independent of the heteroatoms involved, and comparable to the distance found in **1** containing the larger Sn atoms (4.07 Å). In addition we report two metal complexes with square planar [(**4**)$PtCl_2$] (**4-Pt**) and octahedral *cis*-[(**4**)$Mo(CO)_4$] (**4-Mo**) geometries. In both complexes the bis(phosphine) backbone is distorted, but notably less so than in bis(sulfide) **4-S**. All compounds were fully characterized, and except for bis(phosphine) **5**, crystal structures were determined.

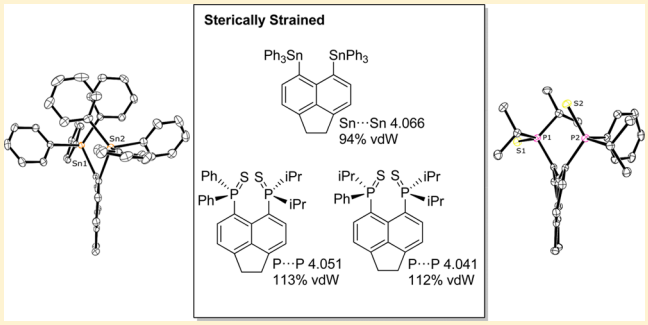

INTRODUCTION

The capability for naphthalene and related polycyclic aromatic hydrocarbons to accommodate atoms or groups larger than hydrogen at the proximal *peri*-positions, at distances well within the sum of their van der Waals radii, stems from their ability to minimize steric strain, and thus achieve a relaxed geometry, by either distorting the usually rigid carbon framework or by forming a direct bond between the *peri*-substituents.[1,2] Naturally, when larger atoms are constrained in this cramped environment they suffer greater steric hindrance as a result of increased repulsive nonbonding interactions between overlapping orbitals, leading to greater deformation of the organic backbone and subsequently longer *peri*-distances.[1−3] The number, size, and nature of the functional groups bound to the *peri*-atoms, and the type of organic backbone employed, however, can also determine the degree of strain present in these systems, and impose large separations between the closely aligned *peri*-atoms. This is aptly demonstrated by comparing the compounds of Figure 1, the only *peri*-substituted systems reported up until now with separations larger than 3.8 Å.[4−11]

Interestingly, the largest separation is found between phosphorus atoms in tris(sulfide) **A** [4.072(3) Å],[4,11] with similar values observed for bis(phosphorus) **B**−**D**,[5−7,11] despite compounds with much larger *peri*-heteroatoms having been prepared (for example **E**−**H**).[2,8,9,11] In these compounds, P···P separations are remarkably 6−13% longer than the sum of van der Waals radii and can be explained by the increased crowding of the bay-region by the introduction of bulky chalcogen atoms in **A**−**C**[4−6] and the severe Coulombic repulsion experienced by the closely aligned positively charged phosphorus centers in **D**.[7] The series of 1,8-bis(trimethylelement)naphthalenes **F**−**H** represents a set of equally strained molecules, and in spite of having larger heteroatoms at the proximal *peri*-positions [r_{vdW} (Sn) 2.17 Å, (Ge) 2.11 Å; (Si) 2.10 Å; *cf.* (P) 1.80 Å][12] these molecules display marginally shorter nonbonded distances than **A**−**D**.[9] With all three compounds adopting the same conformation in the solid, bis(stannane) derivative **F** incorporating the larger congener unsurprisingly exhibits the largest *peri*-separation [3.864 Å], with shorter but comparable distances observed for the lighter elements of the group [**G** 3.809 Å; **H** 3.803 Å].[9] In each case, the separation represents a distance ∼10% shorter than the sum of van der Waals radii. In contrast, the corresponding C···C separation in 1,3,6,8-tetra-*tert*-butylnaphthalene **I** is 14% longer than twice the van der Waals radius of C (3.4 Å)[12] and at 3.861 Å is comparable to the

Received: June 20, 2014
Published: July 31, 2014

   dx.doi.org/10.1021/ic5014768 | *Inorg. Chem.* 2014, 53, 8795−8808

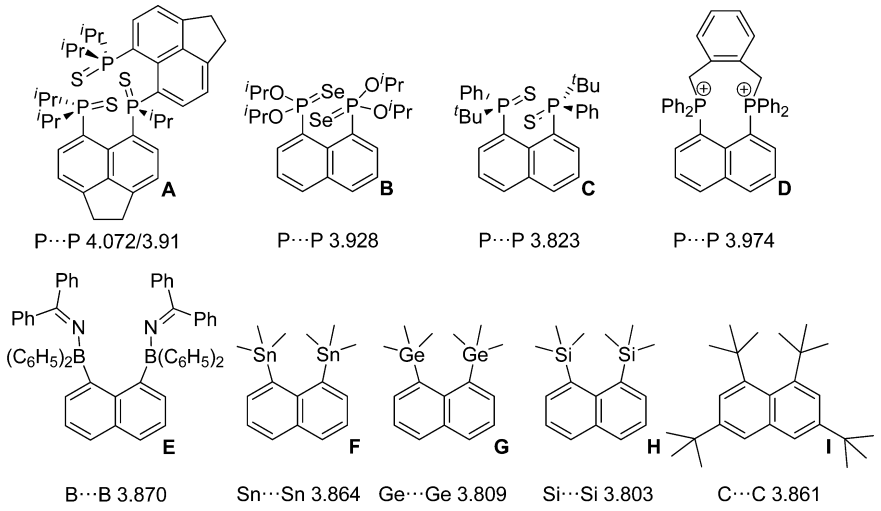

Figure 1. Severely strained *peri*-substituted systems incorporating nonbonded distances greater than 3.8 Å.[4−10]

Sn···Sn distance observed in bis(stannane) **F**.[9,10] This is attributed to the differing alignment of the two *peri*-substituted *tert*-butyl groups rather than the presence of additional groups in the 3 and 6 positions.[10]

The extent of repulsion operating in the bay-region between *peri*-functionalities is thus dictated by a number of structural factors, all of which combine to determine the degree of molecular distortion required to relieve the buildup of steric strain and achieve a minimum energy geometry.[1,2] Under certain geometric conditions, however, attractive noncovalent intramolecular interactions, involving lone-pair orbitals, are known to counterbalance the repulsion between heavier congeners in sterically crowded systems and thus play an important role in controlling their fine structures.[2,13−16] For example, in bis(telluride) **J**[17] and tin−phosphorus derivative **K**,[18] the delocalization of a lone-pair to an antibonding σ^*(E−C) orbital, forms a donor−acceptor three-center four-electron (3c-4e) type interaction, leading to *peri*-distances significantly shorter than the sum of van der Waals radii (**J** 3.3674(19) Å, $\sum r_{vdW}$ 4.12 Å; **K** 2.815(3) Å, $\sum r_{vdW}$ 3.97 Å; Figure 2).[12,17,18] Similar lp(E) → *p*(B) donor−acceptor interactions are observed in boron−chalcogen systems of type **L** and to a lesser extent in their cationic derivatives **M**, with electron donation from the chalcogen moiety notably shortening the intramolecular B···E distance and subsequently reducing the electron deficiency of the boron center.[19] The effects of steric repulsion are similarly reduced by employing a second rigid organic backbone, which imposes additional geometric constraints on the molecule and adds extra stabilization by incorporating the *peri*-atoms into a central heterocyclic ring system.[20−22] This is illustrated by the notable reduction in *peri*-distance by 0.3−0.4 Å for cyclic 1,8-naphthalenediyl compounds **N** and **O** (Figure 2)[21,22] compared to the corresponding distances in strained 1,8-bis(trimethylelement)-naphthalenes **F**−**H** (Figure 1).[9] Furthermore, the aforementioned proximity of the *peri*-atoms in *peri*-substituted systems allows compounds with a stabilizing bridging geometry to be formed (for example **P**, **Q**; Figure 2)[23,24] and specifically bidentate coordination to a metal center to create a chelate ring (for example **R**).[25,26]

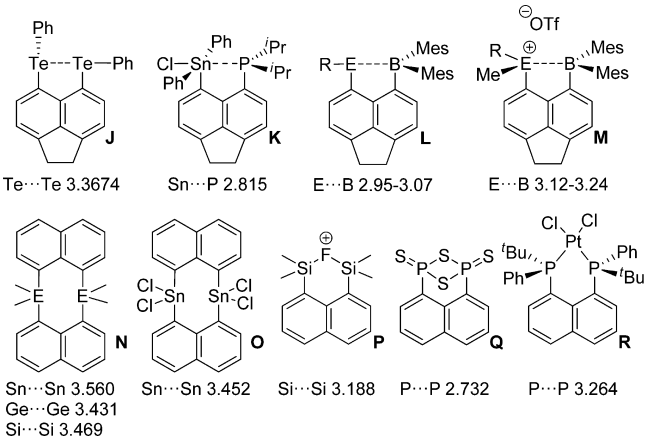

Figure 2. Stabilization of large heteroatoms and groups in *peri*-substituted systems via weak attractive interactions, additional rigid backbone, bridging geometries, and metal complexation.[17−19,21−26]

In the present study, we explore the relationship between attraction and repulsion occurring within sub-van der Waals distances in a number of sterically restricted *peri*-substituted systems. Herein we report the synthesis and structural study of severely strained acenaphthenes **1**−**3** incorporating bulky tin−tin moieties in the proximal positions ([Acenap$(SnR_3)_2$] Acenap = acenaphthene-5,6-diyl; R_3 = Ph_3 (**1**), Me_3 (**2**); [(Acenap)$_2$$(SnMe_2)_2$] (**3**))[27] and compare the degree of repulsion in these systems to heteroleptic bis(phosphines) **4** and **5** ([Acenap$(PR_2)(P^iPr_2)$] R_2 = Ph_2 (**4**), Ph(^{i}Pr) (**5**)), their respective strained bis(sulfide) derivatives **4-S** and **5-S** ([Acenap$(P(=S)R_2)(P(=S)^iPr_2)$] R_2 = Ph_2 (**4-S**), Ph(^{i}Pr) (**5-S**)) and metal complexes [(**4**)$PtCl_2$] (**4-Pt**) and *cis*-[(**4**)$Mo(CO)_4$] (**4-Mo**) (Figure 3).

RESULTS AND DISCUSSION

Bis(acenaphth-5,6-yl)trialkyltin derivatives 1−3: Bis(stannanes) [Acenap$(SnR_3)_2$] **1**−**3** were prepared following a procedure similar to that used previously in the preparation of comparable bis(chalcogen) systems.[17] For their synthesis, the *N*,*N*,*N*′,*N*′-tetramethyl-1,2-ethanediamine (TMEDA) complex of 5,6-dilithioacenaphthene was treated with 2 equiv of the respective triorganotin chloride [Ph_3SnCl, Me_3SnCl, Me_2SnCl_2] to afford [Acenap$(SnPh_3)_2$] (**1**), [Acenap$(SnMe_3)_2$] (**2**), and [(Acenap)$_2$$(SnMe_2)_2$] (**3**) in moderate to good yield [48 (**1**), 65 (**2**), 60% (**3**); Scheme 1]. All three compounds

dx.doi.org/10.1021/ic5014768 | Inorg. Chem. 2014, 53, 8795−8808

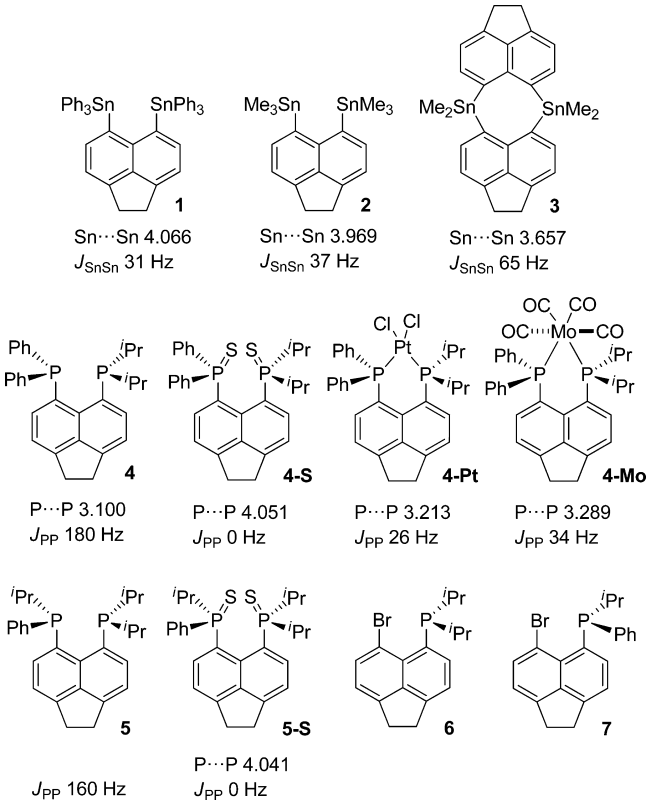

Figure 3. Sterically crowded bis(stannanes) **1**–**3**, bis(phosphines) **4** and **5**, strained bis(sulfides) **4-S** and **5-S**, metal complexes **4-Pt** and **4-Mo** and bromine–phosphorus precursors **6**[16] and **7**.

Scheme 1. Preparation of 5,6-Bis(trialkyltin)acenaphthenes 1–3 via 5,6-Dilithioacenaphthene–TMEDA Complex[a]

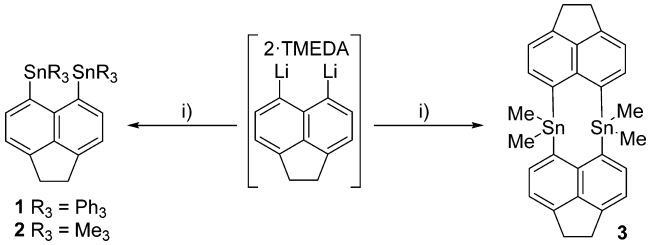

[a]Conditions: (i) Ph_3SnCl (**1**); Me_3SnCl (**2**); Me_2SnCl_2 (2 equiv) (**3**); Et_2O, −10 °C, 1 h.

were characterized by multinuclear magnetic resonance spectroscopy and mass spectrometry, and the homogeneity of the new compounds was confirmed by microanalysis. ^{119}Sn NMR spectroscopic data for the series is displayed in Table 1.

The ^{119}Sn{^{1}H} NMR spectra for bis(stannanes) **1**–**3** display single peaks with satellites attributed to ^{119}Sn–^{117}Sn coupling. The NMR signal for triphenyltin derivative **1** (−120.8 ppm) is shifted notably upfield compared to the trimethyltin analogue **2** (−24.3 ppm), and the relatively small $J(^{119}Sn,^{117}Sn)$ values observed for both derivatives (**1** 31 Hz; **2** 37 Hz) suggest only a limited through-space component contributes to the overall $^4J_{SnSn}$ coupling in these systems. This is in line with the notably large Sn···Sn *peri*-separations observed in the solid in each case (*vide infra*), and comparable to previously reported $^4J(^{119}Sn,^{117}Sn)$ values for $Me_3Sn(CH_2)_3SnMe_3$ (34.4 Hz) and cyclic 1,1,5,5-tetramethyl-1,5-distannacyclooctane (30.3 Hz).[28] As expected, the δ_{119Sn} for the cyclic derivative **3** (−60.3 ppm) lies between the values for **1** and **2**, shifted upfield from the trimethyltin derivative following the replacement of two methyl groups with the less electron-donating bridging acenaphthene fragment. The greater restriction imposed on the geometry of the *peri*-region in **3** by the presence of two rigid acenaphthene backbones results in a notably shorter *peri*-separation than observed in **1** and **2** (*vide infra*), with transannular Sn···Sn interaction leading to a minor increase in $J(^{119}Sn,^{117}Sn)$ coupling (65 Hz) due to the presence of a small through-space coupling component.

Single crystals suitable for X-ray work were obtained for **1** by diffusion of hexane into a saturated solution of the compound in dichloromethane and for **2** and **3** by recrystallization from THF and chloroform solutions of the respective compounds at −30 °C. All three compounds crystallize with one molecule in the asymmetric unit. Selected interatomic bond lengths and angles are listed in Table 2. Further crystallographic information is listed in the Supporting Information (SI).

Table 2. Selected interatomic distances [Å] and angles [°] for Acenap[SnR_3]$_2$ compounds 1–3

compd	1	2	3
SnR_3	$SnPh_3$	$SnMe_3$	$SnMe_2$
peri-Region-Distances			
Sn(1)···Sn(2)	4.0659(9)	3.9693(6)	3.6574(6)
$\sum r_{vdW}$ - Sn···Sn[a]	0.274	0.371	0.683
$\%\sum r_{vdW}$[a]	94	91	84
Sn(1)–C(1)	2.165(3)	2.163(3)	2.164(5)
Sn(2)–C(9)	2.164(4)	2.160(4)	2.161(6)
peri-Region Bond Angles			
Sn(1)–C(1)–C(10)	128.8(2)	127.6(2)	123.6(4)
C(1)–C(10)–C(9)	129.5(3)	129.5(3)	127.1(5)
Sn(2)–C(9)–C(10)	128.5(2)	127.5(3)	123.1(3)
$\sum$ of bay angles	386.8(4)	384.6(5)	373.8(7)
splay angle[b]	26.8	24.6	13.8
C(4)–C(5)–C(6)	111.1(3)	111.2(3)	111.4(5)
Out-of-Plane Displacement			
Sn(1)	−1.045(1)	1.023(1)	0.962(1)
Sn(2)	0.725(1)	−0.735(1)	−0.845(1)
Central Naphthalene Ring Torsion Angles			
C:(6)–(5)–(10)–(1)	−174.3(3)	173.3(4)	−175.2(5)
C:(4)–(5)–(10)–(9)	−175.7(3)	175.6(4)	−176.5(5)

[a]van der Waals radii used for calculations: r_{vdW}(Sn) 2.17 Å; [b]Splay angle: $\sum$ of the three bay-region angles −360.

Table 1. ^{31}P and ^{119}Sn NMR Spectroscopy Data[a]

	1	2	3		4	5	4-S	5-S	4-Pt	4-Mo
^{119}Sn	−120.8	−24.3	−60.3	^{31}P{^{1}H}	−11.3, −12.8	−9.7, −13.4	82.0, 48.6	79.6, 56.8	13.4, −2.3	43.1, 34.5
J_{SnSn}	31	37	65	J_{PP}	180	160	0	0	26	34

[a]All spectra were run in $CDCl_3$; δ (ppm), J (Hz).

dx.doi.org/10.1021/ic5014768 | Inorg. Chem. 2014, 53, 8795–8808

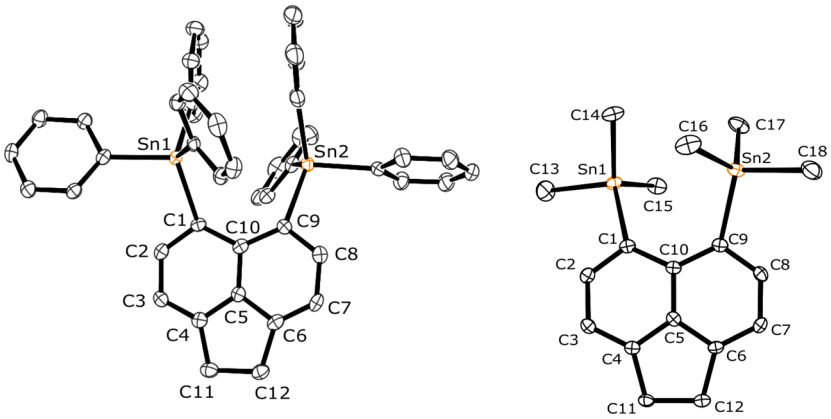

Figure 4. Thermal ellipsoid plots (40% probability) of bis(stannanes) **1** and **2** (H atoms omitted for clarity).

The double substitution of extremely bulky tin moieties at the *peri*-positions in **1** and **2** unsurprisingly causes substantial repulsion and a buildup of steric pressure between the two closely located tin centers as a result of occupied orbital overlap. In order to accommodate such large atoms or groups, severe deformation of the acenaphthene carbon framework is required, with in-plane and out-of-plane distortions and buckling of the aromatic ring system (angular strain) necessary to help partially alleviate steric strain. In both compounds, considerable distortion of the exocyclic C_{Acenap}−Sn bonds within the bay-region is evident from exceptionally large positive splay angles, with the divergence of the *peri*-bonds greater for the bulkier triphenyltin derivative [**1** 26.8°] compared to the smaller trimethyltin analogue [**2** 24.6°] (Figure 4).

Further deformation of the bay geometry is achieved in both cases by substantial displacement of the two *peri*-tin atoms to opposite sides of their respective mean acenaphthene planes by ∼1 Å (Figure 5). In addition to the distortions within the bay-region, both acenaphthene skeletons are notably twisted, resulting in central C−C−C−C torsion angles deviating from planarity by up to 7°. Consequently, exceptionally long nonbonded intramolecular Sn···Sn *peri*-distances are observed in both compounds, with a marginal lengthening of the *peri*-gap for the bulkier triphenyltin moiety **1** [4.0659(9) Å] compared to the trimethyltin analogue **2** [3.9693(6) Å]. The distance of the former is only 6% shorter than twice the sum of van der Waals radii of Sn [4.34 Å][12] and statistically of equal magnitude to the largest *peri*-separation previously reported for a geminally bis(*peri*-substituted) tridentate phosphine tris(sulfide) (Figure 1 **A**; 4.072(3) Å).[4] It is interesting to note that the Sn···Sn distance in **2** is only marginally longer than the *peri*-separation reported for the naphthalene analogue [3.864 Å].[9]

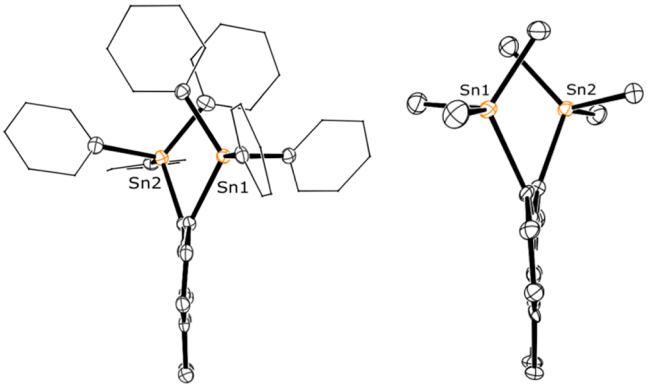

Figure 5. Thermal ellipsoid plots (40% probability) showing the degree of out-of-plane distortion in bis(stannanes) **1** and **2** (phenyl rings in **1** are shown in wireframe, and H atoms are omitted in both cases for clarity).

Strained bis(stannanes) **1** and **2** adopt conformations similar to those of corresponding 1,8-bis(trimethylelement)-naphthalenes **G** (Ge) and **F** (Sn) (Figure 1),[9] with the R_3Sn groups aligning in each case such that a pair of Sn−C bonds, one from each Sn center (Sn1−C3 and Sn2−C37 in **1**; Sn1−C14 and Sn2−C17 in **2**; Figure 6), aligns roughly perpendicular to the mean acenaphthene plane (Figure 6). The severe out-of-plane displacement experienced by the two Sn atoms in both **1** and **2** results in the two perpendicular alkyl groups being in close proximity, in contrast to the distal arrangement of the groups in the carbon analogue of **2**.[9,10] Along with corresponding R_3Sn group conformations, **1** and **2** also exhibit comparable geometries around each tin center, which are best described as distorted tetrahedral; C−Sn−C angles lie in the range 99.64(14)−120.86(15)° and for each tin center average to ∼109° (Table 3).

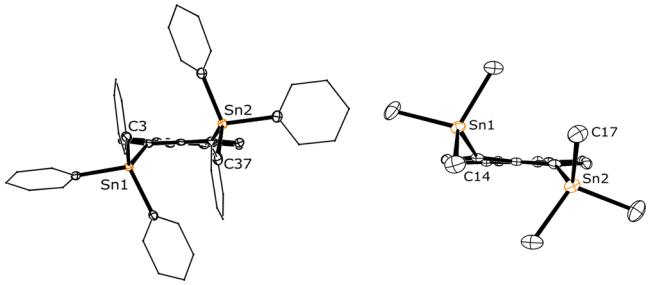

Figure 6. Thermal ellipsoid plots (40% probability) of bis(stannanes) **1** and **2** showing the $(R_3)_3Sn$ group conformations (phenyl rings in **1** are shown in wireframe, and H atoms are omitted in both cases for clarity).

In contrast to bis(stannane) "monomers" **1** and **2**, formed from the reaction of the 5,6-dilithioacenaphthene−TMEDA complex with organotin monochlorides (Ph_3SnCl, Me_3SnCl), treatment of the intermediate with organotin dichloride Me_2SnCl_2 affords a "dimeric" compound **3** in which two dimethyltin groups are linked by two acenaphthene-5,6-diyl ligands to form an 8-membered dimetallacycle (Figure 7). As a consequence of the C_i symmetry (crystallizing in the triclinic $P\bar{1}$

dx.doi.org/10.1021/ic5014768 | Inorg. Chem. 2014, 53, 8795−8808

Table 3. Bond Angles [deg] Categorizing the Geometry around Sn in 1−3

1		2		3	
C(1)−Sn(1)−C(13)	107.87(12)	C(1)−Sn(1)−C(13)	104.87(16)	C(1)−Sn(1)−C(9^{1})	131.21(19)
C(1)−Sn(1)−C(19)	106.69(13)	C(1)−Sn(1)−C(14)	120.04(17)	C(1)−Sn(1)−C(13)	102.8(2)
C(1)−Sn(1)−C(25)	119.43(15)	C(1)−Sn(1)−C(15)	107.74(15)	C(1)−Sn(1)−C(14)	103.28(17)
C(13)−Sn(1)−C(19)	107.31(14)	C(13)−Sn(1)−C(14)	103.4(2)	C(9^{1})−Sn(1)−C(13)	104.03(19)
C(13)−Sn(1)−C(25)	99.64(14)	C(13)−Sn(1)−C(15)	106.9(2)	C(9^{1})−Sn(1)−C(14)	102.3(2)
C(19)−Sn(1)−C(25)	114.93(13)	C(14)−Sn(1)−C(15)	112.77(17)	C(13)−Sn(1)−C(14)	113.4(2)
C(9)−Sn(2)−C(31)	108.84(13)	C(9)−Sn(2)−C(16)	108.10(16)		
C(9)−Sn(2)−C(37)	120.86(15)	C(9)−Sn(2)−C(17)	115.61(17)		
C(9)−Sn(2)−C(43)	104.31(13)	C(9)−Sn(2)−C(18)	104.84(16)		
C(31)−Sn(2)−C(37)	115.51(14)	C(16)−Sn(2)−C(17)	116.35(18)		
C(31)−Sn(2)−C(43)	104.97(15)	C(16)−Sn(2)−C(18)	105.0(2)		
C(37)−Sn(2)−C(43)	99.98(13)	C(17)−Sn(2)−C(18)	105.75(19)		

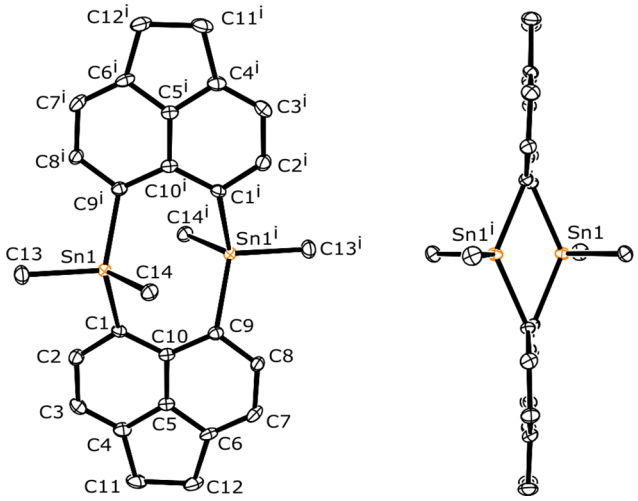

Figure 7. Thermal ellipsoid plots (40% probability) of cyclic bis(stannane) 3 (H atoms are omitted for clarity).

space group) only one crystallographically independent acenaphthene fragment exists within the asymmetric unit, and similarly only a single crystallographically unique tin environment is present.

In the crystal, 3 adopts a conformation similar to that of its naphthalene analogue,[21] aligning the two acenaphthene carbon skeletons on the same plane and displacing the bridging dimethyltin groups to opposite sides of the molecule. As a result, the central 8-membered distannacycle is forced to adopt a chairlike arrangement with two methyl groups (C13/C13^{i}) occupying equatorial positions and two (C14/C14^{i}) located axially (Figure 8). The presence of a single methyl group

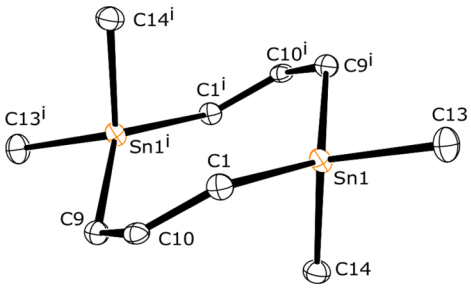

Figure 8. Thermal ellipsoid plot (40% probability) showing the chair conformation of the 8-membered distannacycle in 3 (H atoms are omitted for clarity).

resonance in the ^{1}H NMR spectrum of 3, however, suggests a ring-inversion process takes place in solution, as predicted for the naphthalene analogue.[21] Similar to 1 and 2, the single tin environment in 3 exhibits distorted tetrahedral geometry, although with more obtuse C−Sn−C angles in the range 102.3(2)−131.21(19)°, which average to 110°.

The geometrical constraints present in the structure of 3 imposed by the two rigid acenaphthene backbones fix the dimethyltin moieties in close proximity. The reduced freedom of the now cyclic C_{Acenap}−Sn *peri*−bonds results in a marked decrease in in-plane distortion compared with trimethyltin derivative 2, with the splay angle notably compressed from 24.6° (2) to 13.8° (3) as the tin centers are held more closely together. Further reduction in the distortion of the acenaphthene geometry upon cyclization in 3 is evident from reduced C−C−C−C central torsion angles (~5°) which indicate an increase in the planarity of the carbon skeleton. Nevertheless, the degree of out-of-plane displacement in 3 is consistent with that of its monomeric analogue, with the two tin atoms displaced to opposite sides of each acenaphthene mean plane by up to 1 Å (Figure 7). The significant reduction in in-plane distortion upon cyclization of 3 indicates that the *peri*-atoms are fixed more closely together than in the corresponding monomer, and indeed the nonbonded transannular Sn···Sn *peri*-separation across the distannacycle [3.6374(6) Å] is notably shorter than the equivalent distance in 2 [3.9693(6) Å], although slightly longer than in the naphthalene analogue [3.56 Å].[21]

Bis(phosphines) 4 and 5 and Their Bis(sulfides) 4-S and 5-S: Heteroleptic bis(phosphines) [Acenap(PR$_2$)(P^{i}Pr$_2$)] 4 and 5 were prepared through stepwise halogen−lithium exchange reactions of previously reported 5-(bromo)-6-(diisopropylphosphino)acenaphthene [Acenap(Br)(P^{i}Pr$_2$)] (6)[16] and novel 5-(bromo)-6-(isopropylphenylphosphino)-acenaphthene [Acenap(Br)(PPh^{i}Pr)] (7), respectively. 7 was synthesized following standard literature procedure in moderate yield (40%), starting from 5,6-dibromoacenaphthene[29] and ClP(Ph)^{i}Pr; the synthesis of the latter is omitted from this manuscript but is included in the SI for completeness. Crystals of 6 and 7 suitable for X-ray crystallography were grown from ethanol; the structures of 6 and 7 are shown in Figure 9, and selected bond lengths and angles are given in Table S4 (in the SI).

For the synthesis of 4 and 5, the two bromine precursors 6 and 7 were independently treated with a single equivalent of *n*-butyllithium in diethyl ether under an oxygen and moisture-free nitrogen atmosphere, at −78 °C. Without isolation, addition of

dx.doi.org/10.1021/ic5014768 | Inorg. Chem. 2014, 53, 8795−8808

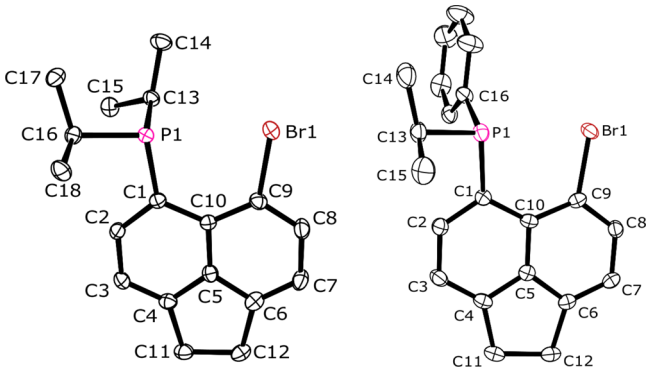

Figure 9. Thermal ellipsoid plots (40% probability) of [Acenap(Br)(P^iPr_2)] (**6**) (left) and [Acenap(Br)(PPh^{i}Pr)] (**7**) (right) (H atoms are omitted for clarity).

the respective chlorophosphine [$ClPPh_2$, ClP^iPr_2] at the same reaction temperature subsequently afforded [Acenap(PPh_2)(P^iPr_2)] (**4**) and [Acenap(PPh^{i}Pr)(P^iPr_2)] (**5**) in good yields [87 (**4**), 78% (**5**), Scheme 2]. Further treatment of phosphines **4** and **5** with 2 equiv of elemental sulfur in refluxing toluene over 3 h afforded the corresponding bis(sulfides) **4-S** and **5-S** in good yield [77% (**4-S**), 85% (**5-S**), Scheme 2].

Scheme 2. Preparation of Heteroleptic Bis(phosphines) [Acenap(PR_2)(P^iPr_2)] 4 and 5 and Their Corresponding Bis(sulfides) 4-S and 5-S[a]

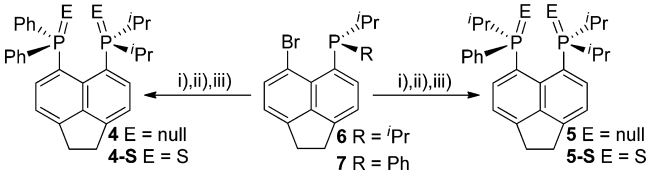

[a]Conditions: (i) *n*BuLi (1 equiv), Et_2O, −78 °C, 1 h; (ii) $ClPPh_2$ (**4**)/ClP^iPr_2 (**5**) (1 equiv), Et_2O, −78 °C, 1 h; then RT (iii) S (2 equiv), toluene, reflux, 3 h.

The $^{31}P\{^1H\}$ NMR spectra of bis(phosphines) **4** (δ_A = −11.3 ppm, δ_B = −12.8 ppm, J_{AB} = 180 Hz) and **5** (δ_A = −9.7 ppm, δ_B = −13.4 ppm, J_{AB} = 160 Hz) reveal expected pseudoquartets associated with typical AB spin systems, both of which correlate well with simulated coupling patterns (Figures S1 and S5, in the SI). The relatively large J_{PP} coupling present in both systems (**4** 180 Hz, **5** 160 Hz) is indicative of a considerable through-space interaction through the phosphorus lone-pairs, which is notably absent in bis(sulfides) **4-S** and **5-S** following oxidation of the phosphorus centers from P^{III} to P^V (Figures S2 and S6, in the SI). In the ^{31}P NMR (^1H coupled) spectra of both compounds additional splitting from the hydrogens of the isopropyl groups is observed, with the signal for P_A (P^iPr_2) now appearing as a doublet of doublets of septets in both **4** (δ_P = −11.3 ppm, J_{PP} = 180 Hz, $^2J_{PH}$ = 24.5 Hz, $^3J_{PH}$ = 11.8 Hz) and **5** (δ_P = −9.7 ppm, J_{PP} = 160 Hz, $^2J_{PH}$ = 25.4 Hz, $^3J_{PH}$ = 12.8 Hz) and the resonance for P_B (PPh^{i}Pr) in **5** displaying as a broad doublet.

Yellow crystals of **4** suitable for X-ray crystallography were obtained from a saturated solution of the compound in acetonitrile at −30 °C, while recrystallization by diffusion of hexane into saturated solutions of the respective compound in dichloromethane afforded colorless blocks of **4-S** and **5-S**. All three compounds crystallize with one molecule in the asymmetric unit. Selected interatomic bond lengths and angles are listed in Table 4. Further crystallographic information can be found in the SI. Growing crystals of **5** was attempted using various techniques but was unsuccessful.

Within the molecular structure of bis(phosphine) **4**, the two P−C_{Ph} bonds adopt perpendicular (type A) and coplanar (type B) alignments with respect to the mean acenaphthene plane,[13,17] with the latter affording a *quasi*-linear C_{Ph}−P···P three-body fragment that has the potential to promote the delocalization of the phosphorus lone-pair of the P($^iPr_2$) group to an antibonding σ^*(P−C_{Ph}) orbital on the opposite side of the *peri*-gap.[17,18] Conveniently, the two isopropyl groups occupy positions on opposite sides of the acenaphthene plane with an axial-twist configuration (type AC)[13,30] that orientates

Table 4. Selected Interatomic Distances [Å] and Angles [deg] for 4, 4-S, 4-Pt, 4-Mo, and 5-S

cmpd	4	4-S	4-Pt	4-Mo	5-S
peri-Region Bond Distances					
P(1)···P(2)	3.100(2)	4.051(2)	3.213(6)	3.289(1)	4.041(1)
$\sum r_{vdW}$ - P···P[a]	0.500	−0.451	0.387	0.311	−0.441
% $\sum r_{vdW}$[a]	86	113	89	91	112
P(1)−C(1)	1.851(5)	1.850(6)	1.818(14)	1.836(4)	1.853(4)
P(2)−C(9)	1.862(4)	1.849(5)	1.780(14)	1.843(4)	1.828(3)
peri-Region Bond Angles					
P(1)−C(1)−C(10)	121.8(3)	127.4(4)	124.8(10)	122.7(3)	126.3(3)
C(1)−C(10)−C(9)	128.8(4)	132.6(5)	128.5(12)	130.0(4)	131.7(3)
P(2)−C(9)−C(10)	123.7(4)	127.2(4)	121.1(10)	126.0(3)	126.2(2)
$\sum$ of bay angles	374.3(8)	387.2(8)	374.4(19)	378.7(6)	384.2(5)
splay angle[b]	14.3	27.2	14.4	17.7	24.2
C(4)−C(5)−C(6)	110.8(4)	110.9(5)	110.3(13)	110.1(4)	110.6(3)
Out-of-Plane Displacement					
P(1)	0.233(1)	0.989(1)	0.453(1)	0.337(2)	1.179(1)
P(2)	−0.053(1)	−1.206(1)	−0.689(1)	−0.359(2)	−1.218(1)
Central Naphthalene Ring Torsion Angles					
C:(6)−(5)−(10)−(1)	178.3(4)	−163.3(5)	177.7(11)	175.2(4)	−164.6(3)
C:(4)−(5)−(10)−(9)	−177.2(4)	−167.4(5)	169.5(11)	176.5(4)	−164.7(3)

[a]van der Waals radii used for calculations: r_{vdW}(P) 1.80 Å. [b]Splay angle: $\sum$ of the three bay-region angles −360°.

dx.doi.org/10.1021/ic5014768 | *Inorg. Chem.* 2014, 53, 8795−8808

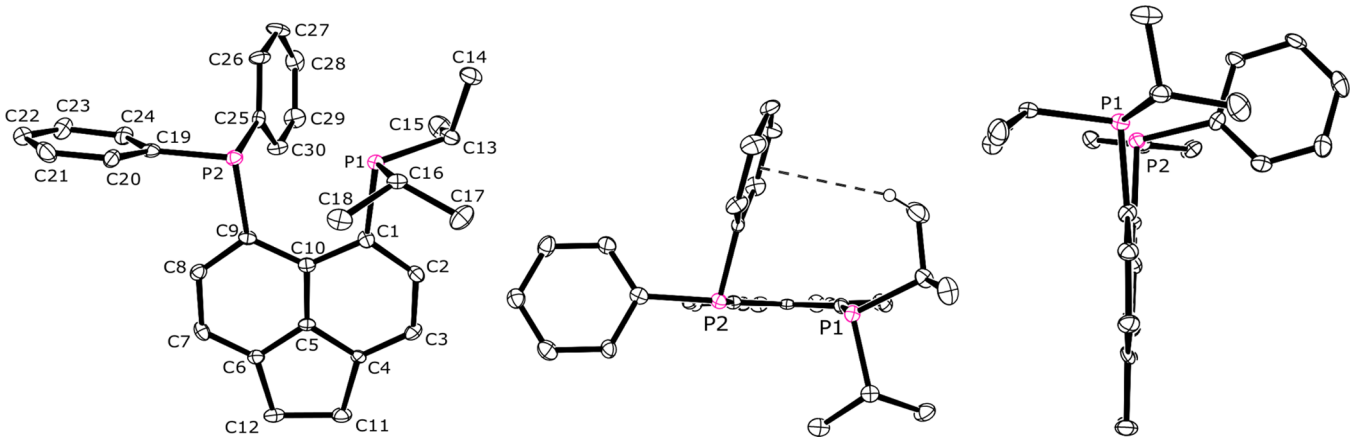

Figure 10. Thermal ellipsoid plots (40% probability) of bis(phosphine) **4** showing the conformation of the PR_2 groups and CH···π interaction (middle) and the degree of out-of-plane distortion (right) (all but one H atoms are omitted for clarity).

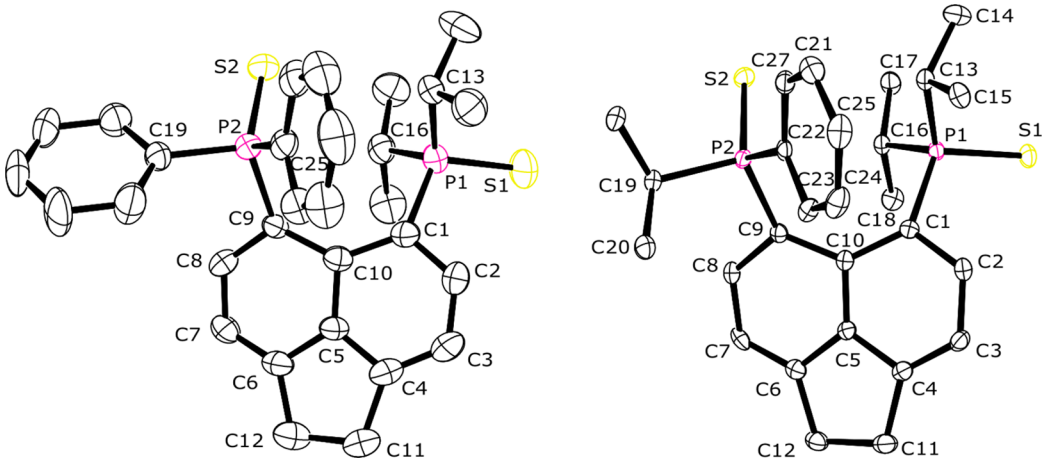

Figure 11. Thermal ellipsoid plots (40% probability) of strained bis(sulfides) **4-S** and **5-S** (H atoms are omitted for clarity).

the lone-pair of the P(^{i}Pr$_2$) group pointing directly at the opposing phosphorus atom across the bay (Figure 10).

In conjunction with the notably large J_{PP} through-space coupling (180 Hz) observed in the $^{31}P\{^1H\}$ NMR spectrum of **4**, the notably short intramolecular P···P distance (3.100(2) Å; 14% shorter than twice the van der Waals radius of P) and the close to linear C_{Ph}–P···P angle of 175.65(1)° provide further support for a weakly attractive three-center four-electron (3c-4e) type interaction operating between the *peri*-atoms in this system. Along with the additional stabilization provided by an intramolecular CH···π interaction between adjacent isopropyl and phenyl groups [H15B···Cg(25–30) 3.137(1) Å; Figure 10, Table S5, in the SI], these weakly attractive intramolecular forces help to counterbalance the steric repulsion of the two phosphorus atoms and thus reduce the degree of molecular distortion within the acenaphthene framework. Consequently, the organic backbone shows only a minor deviation from planarity with maximum central C–C–C–C torsion angles *ca.* 2° and a standard deviation from the mean plane of only 0.02 Å. In addition, P(2) essentially lies on the mean plane with P(1) experiencing only a minor out-of-plane distortion, displaced by only 0.2 Å (Figure 10). The most significant deformation of the acenaphthene geometry occurs within the plane of the molecule where the exocyclic P–C_{Acenap} bonds diverge with a splay angle of 14.3°.

As anticipated, the crystal structures of **4-S** and **5-S** (Figure 11) are considerably more strained than that of **4**, due to the excessive overcrowding of the bay-region caused by the increased bulk of the phosphorus moieties upon thionation. Repulsive forces dominating these systems induce dramatic buckling of the carbon framework and extreme displacement of the exocyclic *peri*-bonds. Maximum C–C–C–C central acenaphthene torsion angles of ∼17° (*cf.* 3° for **4**) illustrate the degree to which the rigid organic scaffolds have been twisted from their naturally planar environment, with the out-of-plane distortions resulting in displacement of the two phosphorus atoms in each case by ∼1.2 Å (Figure 12). In the same vein, splay angles in the bay-region are substantially more obtuse in **4-S** [27.2°] and **5-S** [24.2°] than in **4** [14.3°] due to the exocyclic P–C_{Acenap} bonds tilting further apart to minimize the steric collisions.

Additional distortion of the carbon skeleton involves widening of the C1–C10–C9 bay-angle (mean 132° *cf.* ideal 127°),[31] elongation of the bonds around C10 (average lengths 1.45 Å *cf.* ideal 1.42 Å) and stretching of the central C5–C10 bond from 1.39 Å to an average of 1.41 Å, although it is worth noting that despite the extensive deformations occurring at the top of the molecule closest to the repulsive interactions, the presence of the ethylene bridge ensures the bonds around C5 retain their ideal length (average 1.42 Å) and the C4–C5–C6 angle remains at 111°.

dx.doi.org/10.1021/ic5014768 | *Inorg. Chem.* 2014, 53, 8795–8808

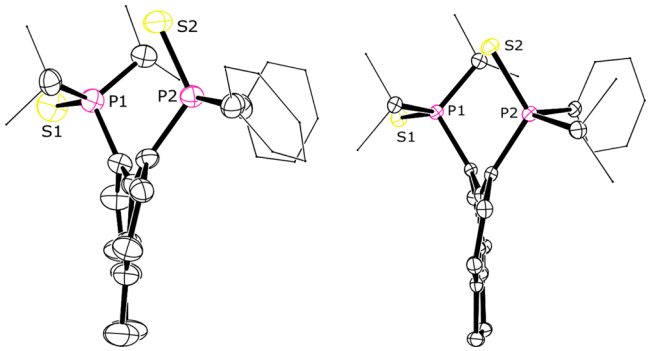

Figure 12. Thermal ellipsoid plots (40% probability) of strained bis(sulfides) **4-S** and **5-S** illustrating the extent of out-of-plane distortion and buckling of the acenaphthene framework (H atoms are omitted and Ph and ^{i}Pr groups are shown in wireframe for clarity).

The overall degree of molecular distortion occurring in **4-S** and **5-S** is best quantified by considering the magnitude of the nonbonded intramolecular P···P distances, which at 4.051(2) Å (**4-S**) and 4.041(1) Å (**5-S**) are considerably longer (~13%) than the sum of van der Waals radii of two P atoms (3.60 Å).[12] These distances are comparable to the distance found in **1** containing the much larger Sn atoms [4.0659(9) Å], and are among the largest ever reported *peri*-separations, independent of the heteroatoms involved.[11]

Similar to strained bis(stannanes) **1** and **2**, the S═PR$_2$ groups in **4-S** and **5-S** are located such that a pair of P−Z bonds (P═S on P(2); P−C$_{iPr}$ on P(1)) align roughly perpendicular to the mean acenaphthene plane (Figure 13).

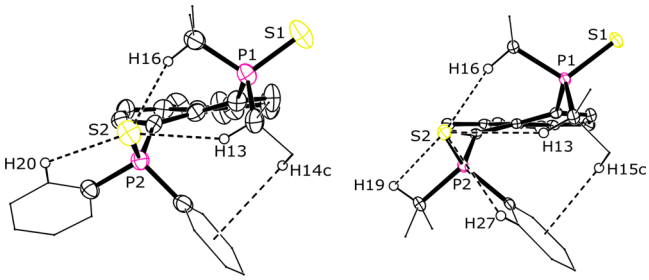

Figure 13. Thermal ellipsoid plots (40% probability) of strained bis(sulfides) **4-S** and **5-S** showing the conformation of the S═PR$_2$ groups (majority of H atoms are omitted and Ph and ^{i}Pr groups are shown in wireframe for clarity).

The extent of the out-of-plane distortion, concomitant with the buckling of the carbon framework in both compounds, results in the sulfur atoms on each P(2) aligning close to the isopropyl groups on the adjacent phosphorus atoms, allowing for C−H···S type weak hydrogen bonds to exist across the *peri*-gap in each case [H13···S(2) **4-S** 2.691(1) Å, **5-S** 2.864(1) Å; H16···S(2) **4-S** 2.678(1) Å, **5-S** 2.676(1) Å; Figure 13, Table S5, in the SI]. Additional C−H···S close contacts are observed between S(2) and the isopropyl and phenyl rings on P(2) [**4-S** H20···S(2) 2.720(1) Å; **5-S** H21C···S(2) 2.868(1) Å, H27···S(2) 2.922(1) Å; Figure 13, Table S5, in the SI]. The proximal arrangement of the phosphorus moieties also places a phenyl ring on P(2) in close contact with the axial isopropyl group on P(1) such that an additional CH···π interaction acts to further stabilize this conformation [**4-S** H14···Cg(25−30) 3.008(1) Å; **5-S** H15···Cg(22−27) 2.688(1) Å; Figure 13, Table S5, in the SI].

Platinum(II) (4-Pt) and Molybdenum(0) (4-Mo) Complexes of Bis(phosphine) 4: Treatment of bis(phosphine) **4** with PtCl$_2$(cod) (cod =1,5-cyclooctadiene) in CH$_2$Cl$_2$ at room temperature, followed by removal of the volatiles by evaporation, afforded the monomeric, mononuclear [{Acenap-(PPh$_2$)(P^{i}Pr$_2$)}{PtCl$_2$}] complex **4-Pt** as a white solid in excellent yield (87%; Scheme 3). The corresponding reaction

Scheme 3. Coordination Chemistry of Bis(phosphine) 4: Preparation of [{Acenap(PPh$_2$)(P^{i}Pr$_2$)}{PtCl$_2$}] (4-Pt) and [{Acenap(PPh$_2$)(P^{i}Pr$_2$)}{MoCO$_4$}] (4-Mo)[a]

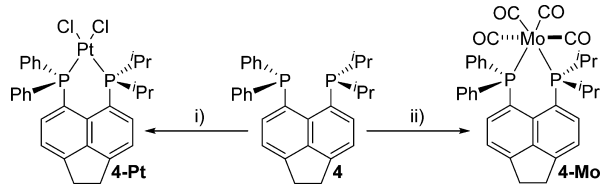

[a]Conditions: (i) [PtCl$_2$(cod)], CH$_2$Cl$_2$, RT, 12 h; (ii) [(nbd)Mo-(CO)$_4$], CH$_2$Cl$_2$, RT, 12 h.

of **4** with [(nbd)Mo(CO)$_4$] (nbd = norbornadiene) under the same reaction conditions afforded [{Acenap(PPh$_2$)(P^{i}Pr$_2$)}-{Mo(CO)$_4$}] **4-Mo** as a brown solid in good yield (60%; Scheme 3).

The ^{31}P{^{1}H} NMR spectrum of **4-Pt** exhibits two doublets at δ_P 13.4 ppm (P^{i}Pr$_2$) and −2.3 ppm (PPh$_2$) ($^{2}J_{PP}$ = 26.1 Hz), each accompanied by a set of satellites attributed to ^{31}P−^{195}Pt coupling ($^{1}J_{PPt}$ = 3352 Hz (P^{i}Pr$_2$) and 3407 Hz (PPh$_2$); Figure S3, in the SI). The single resonance in the ^{195}Pt{^{1}H} NMR spectrum appears as an anticipated doublet of doublets, centered at δ_{Pt} −4504.1 ppm, with $^{1}J_{PPt}$ coupling constants correlating to the values found in the ^{31}P{^{1}H} NMR spectrum (Figure S4, in the SI). While the ^{31}P (^{1}H coupled) NMR spectrum of **4-Pt** displays additional splitting from the coupling to the isopropyl hydrogens, the overlap of peaks prevents the J_{PH} coupling from being determined. The coupling can be observed, however, in the ^{1}H NMR spectrum, which reveals two doublets of septets for the two magnetically inequivalent PC*H* hydrogen environments ($^{2}J_{HP}$ = 18.6 Hz, $^{3}J_{HH}$ = 7.0 Hz; $^{2}J_{HP}$ = 16.5 Hz, $^{3}J_{HH}$ = 5.5 Hz) and a pair of doublet of doublets for the inequivalent methyl groups ($^{3}J_{HP}$ = 17.9 Hz, $^{3}J_{HH}$ = 7.0 Hz; $^{3}J_{HP}$ = 16.2 Hz, $^{3}J_{HH}$ = 7.0 Hz). Correspondingly, the ^{31}P{^{1}H} NMR spectrum of **4-Mo** revealed two doublets at δ_P 43.1 ppm (P^{i}Pr$_2$) and 34.5 ppm (PPh$_2$) ($^{2}J_{PP}$ = 33.5 Hz). Similar to **4-Pt** the ^{1}H NMR spectrum enabled J_{PH} coupling to the isopropyl hydrogens to be determined; however, due to the overlap of resonances this was only possible for the magnetically inequivalent methyl groups represented by a pair of doublet of doublets ($^{3}J_{HP}$ = 14.9 Hz, $^{3}J_{HH}$ = 6.9 Hz; $^{3}J_{HP}$ = 15.8 Hz, $^{3}J_{HH}$ = 7.0 Hz).

Colorless crystalline blocks of **4-Pt** and yellow platelet crystals of **4-Mo** suitable for X-ray crystallography were grown from diffusion of hexane into a saturated solution of the respective products in dichloromethane. The crystal structures of **4-Pt** and **4-Mo** are shown in Figure 14, and selected interatomic bond lengths and angles are listed in Table 4. Further crystallographic information can be found in the SI.

The structures of related monomeric platinum(II) **4-Pt** and molybdenum(0) **4-Mo** complexes both involve bidentate P/P coordination of the unsymmetrical bis(phosphine) ligand **4** to form six-membered chelate rings involving the central metal

dx.doi.org/10.1021/ic5014768 | Inorg. Chem. 2014, 53, 8795−8808

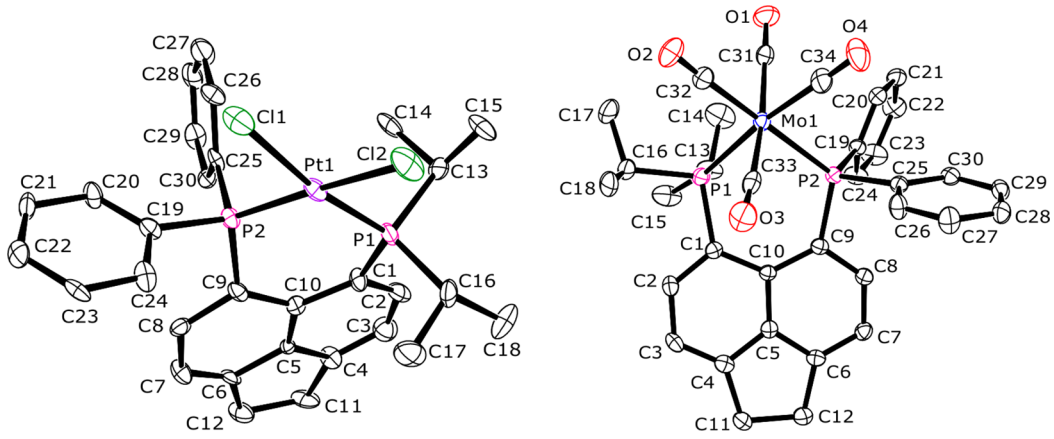

Figure 14. Thermal ellipsoid plots (40% probability) of platinum(II) **4-Pt** and molybdenum(0) **4-Mo** complexes of bis(phosphine) **4** (H atoms are omitted for clarity).

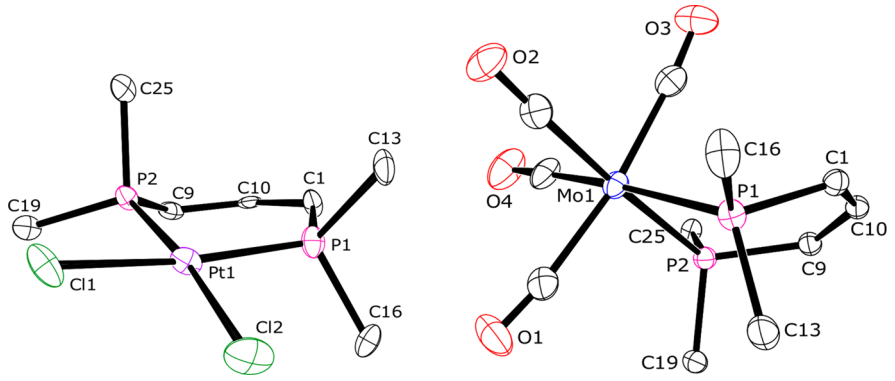

Figure 15. Thermal ellipsoid plots (40% probability) of **4-Pt** and **4-Mo** reduced to their central six-membered MP_2C_3 rings for clarity to show the contrasting distorted boat and twisted envelope conformations, respectively.

Table 5. Bond Lengths [Å] and Angles [deg] Categorizing the Geometry around Pt and Mo in 4-Pt and 4-Mo

4-Pt		4-Mo			
platinum region distances		molybdenum region distances			
P(1)−Pt(1)	2.236(4)	P(1)−Mo(1)	2.5204(11)	Mo(1)−C(32)	1.998(5)
P(2)−Pt(1)	2.203(4)	P(2)−Mo(1)	2.4825(10)	Mo(1)−C(33)	1.998(5)
Pt(1)−Cl(1)	2.349(4)	Mo(1)−C(31)	2.040(5)	Mo(1)−C(34)	1.969(5)
Pt(1)−Cl(2)	2.345(4)				
platinum region angles		molybdenum region angles			
P(1)−Pt(1)−P(2)	92.73(13)	P(1)−Mo(1)−P(2)	82.19(4)	P(2)−Mo(1)−C(34)	89.79(14)
Cl(1)−Pt(1)−Cl(2)	86.78(14)	P(1)−Mo(1)−C(31)	94.94(13)	C(31)−Mo(1)−C(32)	87.70(18)
Cl(1)−Pt(1)−P(2)	90.25(13)	P(1)−Mo(1)−C(32)	100.46(13)	C(31)−Mo(1)−C(33)	171.21(18)
Cl(2)−Pt(1)−P(1)	91.16(14)	P(1)−Mo(1)−C(33)	88.32(13)	C(31)−Mo(1)−C(34)	85.44(19)
Cl(1)−Pt(1)−P(1)	170.55(13)	P(1)−Mo(1)−C(34)	171.97(13)	C(32)−Mo(1)−C(33)	83.67(18)
Cl(2)−Pt(1)−P(2)	173.25(13)	P(2)−Mo(1)−C(31)	96.20(12)	C(32)−Mo(1)−C(34)	87.57(18)
		P(2)−Mo(1)−C(32)	175.11(13)	C(33)−Mo(1)−C(34)	92.48(19)
		P(2)−Mo(1)−C(33)	92.34(13)		

atom. As required by the geometry of the ligand the two phosphine groups adopt a *cis*-orientation around the four-coordinate platinum in **4-Pt** and the six-coordinate molybdenum center in **4-Mo**, which occupy typical square-planar and octahedral coordination environments, respectively.

In **4-Pt** the geometry around the metal center is somewhat distorted, with the phosphorus atoms displaced to opposite sides of the Cl(1)−Pt(1)−Cl(2) plane by up to 0.4 Å, although within the plane angles around Pt lie between 86.78(14)−92.73(13)° and average to 90.2°. As expected, the Pt(1)−P(1) bond distance (2.236(4) Å; P^iPr_2) is marginally longer than the Pt(1)−P(2) distance (2.203(4) Å; PPh_2). This is consistent with an increase in the electronegativity of the phosphine moiety and concomitant increase in the s character of the Pt−P bond, which is mirrored in the ^{31}P NMR with an expected increase in $^1J_{PPt}$ coupling resulting from a shorter bond (Pt−P^iPr_2 3352 Hz; Pt−PPh_2 3407 Hz). The extent of out-of-plane distortion experienced by the two P−C_{Acenap} *peri*-bonds, which is concomitant with a considerable twist of the acenaphthene scaffold, results in the mean Pt(1)−Cl(1)−Cl(2)−P(1)−P(2)

dx.doi.org/10.1021/ic5014768 | Inorg. Chem. 2014, 53, 8795−8808

plane lying at 29° to that of the acenaphthene backbone. In addition, with the phosphorus atoms displaced by up to 0.7 Å from the mean plane and maximum C−C−C−C central torsion angles approaching 11°, the PtP_2C_3 ring is severely buckled and adopts a conformation best described as a distorted boat (Figure 15). The resulting transannular P···P *peri*-distance [3.213(6) Å] is marginally longer than the equivalent distance observed in the free ligand **4** [3.100(2) Å] but considerably shorter than that in bis(sulfide) **4-S** [4.051(2) Å].

The octahedral environment around the molybdenum center in **4-Mo** is marginally distorted, with angles in the range 82.19(4)−100.46(13)° (average 90.1°). In contrast to **4-Pt**, the MoP_2C_3 six-membered chelate ring adopts a twisted envelope-type conformation hinged about the P···P vector, with Mo positioned 1.230(1) Å above the mean P_2C_3 plane and with the P(1)−Mo(1)−P(2) plane inclined by 135° (Figure 15 and Table 5). While the out-of-plane ligand distortions are notably reduced in **4-Mo** compared to those of the platinum complex, greater in-plane displacement of the $P-C_{Acenap}$ *peri*-bonds occurs in order to accommodate the octahedral metal environment, with an increased splay angle of 17.7° and a marginally longer P···P separation [3.289(1) Å] observed compared to those of **4-Pt** [14.4°; 3.213(6) Å].

CONCLUSION

Bis(stannanes) **1**−**3**, incorporating bulky tin moieties in the proximal *peri*-positions on the acenaphthene backbone, have been prepared following standard halogen−lithium exchange reactions giving the *N*,*N*,*N*′,*N*′-tetramethyl-1,2-ethanediamine (TMEDA) complex of 5,6-dilithioacenaphthene and reaction with the respective organotin chloride [Ph_3SnCl, Me_3SnCl, Me_2SnCl_2]. These strained systems are dominated by repulsive forces which result in substantial buckling of the acenaphthene framework and major displacement of the exocyclic *peri*-bonds, leading to intramolecular Sn···Sn distances approaching the sum of van der Waals radii. The distance in triphenyltin derivative **1** [4.0659(9) Å] is only 6% shorter than the sum of van der Waals radii of Sn [4.34 Å][12] and statistically of equal magnitude to the largest *peri*-separation previously reported [4.072(3) Å].[4] The addition of the second acenaphthene fragment in distannacycle **3** acts to partially overcome the repulsion between the two tin atoms, reducing the Sn···Sn distance from 3.9693(6) Å in **2** to 3.6374(6) Å. The relatively large *peri*-distances observed in **1**−**3**, coupled with the small $J(^{119}Sn,^{117}Sn)$ values obtained in the ^{119}Sn NMR spectra, suggest only a limited through-space contribution to the overall coupling in these systems (**1** 31 Hz; **2** 37 Hz; **3** 65 Hz).

Heteroleptic bis(phosphines) [$Acenap(PR_2)(P^iPr_2)$] **4** and **5** have been prepared through stepwise halogen−lithium exchange reactions of bromine−phosphorus precursors [$Acenap(Br)(P^iPr_2)$] (**6**)[16] and [$Acenap(Br)(PPh^iPr)$] (**7**). In the crystal, **4** adopts a conformation incorporating a *quasi*-linear $C_{Ph}-P\cdots P$ three-body fragment with the correct geometry to promote the delocalization of the phosphorus lone-pair of the $P(^iPr_2)$ group to the adjacent antibonding $\sigma^*(P-C_{Ph})$ orbital. The notably short intramolecular P···P distance (3.100(2) Å; 14% shorter than twice the van der Waals radius of P) and the close to linear $C_{Ph}-P\cdots P$ angle of 175.65(1)° suggest a weakly attractive three-center four-electron (3c-4e) type of interaction operates between the *peri*-atoms in this system, which is supported by notably large J_{PP} through-space coupling (180 Hz) observed in the $^{31}P\{^1H\}$ NMR spectrum. A similar interaction is predicted to occur in **5** which exhibits a similar J_{PP} of 160 Hz. Conversely, the corresponding bis(sulfide) derivatives **4-S** and **5-S** prepared by treating the parent bis(phosphines) with elemental sulfur by refluxing in toluene, are highly strained due to the increased crowding of the *peri*-region upon thionation. In each case, extreme in-plane distortion (splay angles up to 27°) is accompanied by severe buckling of the carbon framework (maximum C−C−C−C torsion angles ∼17°), with the phosphorus atoms displaced from the mean acenaphthene plane by up to 1.2 Å. Subsequently, nonbonded intramolecular P···P distances [**4-S** 4.051(2) Å; **5-S** 4.041(1) Å] are considerably longer (∼13%) than the sum of van der Waals radii and are comparable to the largest ever reported *peri*-separations.[11]

Treatment of bis(phosphine) **4** with $PtCl_2(cod)$ (cod =1,5-cyclooctadiene) and $[(nbd)Mo(CO)_4]$ (nbd = norbornadiene) in CH_2Cl_2 at room temperature afforded monomeric, mononuclear complexes [(**4**)$PtCl_2$] (**4-Pt**) and *cis*-[(**4**)$Mo(CO)_4$] (**4-Mo**), with distorted square planar and octahedral metal geometries, respectively. Both complexes involve bidentate P/P coordination of the unsymmetrical, *cis*-orientated bis(phosphine) ligand **4**, which forms a six-membered chelate ring involving the central metal atom. In each case the bis(phosphine) backbone is distorted but notably less so than in bis(sulfide) **4-S**, with comparable P···P distances of 3.213(6) Å and 3.289(1) Å.

EXPERIMENTAL SECTION

All experiments were carried out under an oxygen- and moisture-free nitrogen atmosphere using standard Schlenk techniques and glassware. Reagents were obtained from commercial sources and used as received. Dry solvents were collected from an MBraun solvent system. Elemental analyses were performed at the London Metropolitan University. ^1H, ^{13}C and ^{119}Sn NMR spectra for **1**−**3** were recorded on a Jeol GSX 270 MHz NMR spectrometer with $\delta(H)$, $\delta(C)$, and $\delta(Sn)$ referenced to external tetramethylsilane and tetramethylstannane, respectively. ^1H, ^{13}C, ^{31}P, and ^{195}Pt NMR spectra for **4**, **4-S**, **5-S**, **4-Pt**, **4-Mo** were recorded on a Bruker AVANCE III 500 MHz NMR spectrometer with $\delta(H)$, $\delta(C)$, $\delta(P)$, and $\delta(Pt)$ referenced to external tetramethylsilane, phosphoric acid, and $Na_2(PtCl_6)$, respectively. ^1H, ^{13}C and ^{31}P NMR spectra for **5** were recorded on a Bruker Avance 500 MHz NMR spectrometer with the same external references above. Assignments of ^{13}C and ^1H NMR spectra were made with the help of H−H COSY, HSQC and HMBC experiments. All measurements were performed at 25 °C. All δ values reported for NMR spectroscopy are in parts per million (ppm). Coupling constants (J) are given in Hertz (Hz). All J_{SnSn} values listed in the experimental represent experimentally obtained $J(^{119}Sn,^{117}Sn)$ SSCCs. Mass spectrometry was performed by the University of St. Andrews Mass Spectrometry Service. Electrospray mass spectrometry (ES-MS) was carried out on a Micromass LCT orthogonal accelerator time-of-flight mass spectrometer. 5,6-Dibromoacenaphthene [$AcenapBr_2$][28] and 5-(bromo)-6-(diisopropylphosphino)acenaphthene [$Acenap(Br)(P^iPr_2)$] (**6**)[16] were prepared from standard reported procedures.

[$Acenap(SnPh_3)_2$] (1). A solution of 5,6-dibromoacenaphthene (1.09 g, 3.49 mmol) in diethyl ether (100 mL) was cooled to −10 to 0 °C on an ice−ethanol bath, and to this was added a solution of TMEDA (1.5 mL, 9.44 mmol). The mixture was allowed to stir for 15 min before a solution of *n*-butyllithium (2.5 M) in hexane (3.1 mL, 7.69 mmol) was added dropwise over a period of 15 min. During these operations, the temperature of the mixture was maintained at −10 to 0 °C. The mixture was stirred at this temperature for a further 1 h, before a solution of triphenyltin chloride (2.69 g, 6.98 mmol) in diethyl ether (100 mL) was added dropwise. The mixture was allowed to warm to room temperature and then stirred overnight before being washed with 0.1 M sodium hydroxide (2 × 60 mL). The organic layer

dx.doi.org/10.1021/ic5014768 | Inorg. Chem. 2014, 53, 8795−8808

was dried over magnesium sulfate and concentrated under reduced pressure to afford a cream-colored solid. The crude product was refluxed with hexane for 30 min, affording a white solid precipitate which was collected by filtration. An analytically pure sample was obtained from recrystallization by diffusion of hexane into a saturated solution of the compound in tetrahydrofuran (1.43 g, 48%); mp 180−182 °C. ^{1}H NMR ($CDCl_3$, Me_4Si, 270 MHz) δ_H 7.80 (2H, d, $^{3}J_{HH}$ = 6.9 Hz, $^{3}J_{HSn}$ = 63/59, Acenap 4,7-H), 7.32 (2H, d, $^{3}J_{HH}$ = 6.9 Hz, Acenap 3,8-H), 7.27−7.14 (6H, m, Sn*Ph-p*), 7.14−6.96 (24H, m, Sn*Ph-o,m*), 3.49 (4H, s, Acenap 2 × CH_2); ^{13}C{^{1}H} NMR ($CDCl_3$, Me_4Si, 76 MHz) δ_C 149.4 (q), 142.8 (s, $^{2}J_{CSn}$ = 33 Hz, Acenap 4,7-C), 141.8 (q), 137.3 (s, $^{2}J_{CSn}$ = 36 Hz, Sn*Ph-o*), 134.2 (q), 129.3 (q), 128.8 (q), 128.3 (s, Sn*Ph-p*), 128.2 (s, $^{3}J_{CSn}$ = 52 Hz, Sn*Ph-m*), 119.9 (s, $^{2}J_{CSn}$ = 59 Hz, Acenap 3,8-C), 30.1 (s, Acenap 2xCH_2); ^{119}Sn{^{1}H} NMR ($CDCl_3$, Me_4Sn, 101 MHz) δ_{Sn} −120.8 (s, J_{SnSn} = 31 Hz); MS (ES$^+$): *m/z* (%) 351.02 (70) [$SnPh_3$], 383.05 (100) [$SnPh_3OMe$], 503.08 (30) [$M^+ - SnPh_3$], 875.09 (21) [M + Na]; Anal. Calcd for $C_{48}H_{38}Sn_2$: C, 67.65; H, 4.49. Found: C, 68.07; H, 4.91.

[Acenap(SnMe$_3$)$_2$] (2). Experimental details were the same as for compound **1** but with [Acenap(Br)$_2$] (1.03 g, 3.31 mmol), TMEDA (1.4 mL, 8.93 mmol), 2.5 M solution of *n*-butyllithium in hexane (2.9 mL, 7.28 mmol) and Me_3SnCl (1.7 mL, 1.32 g, 6.62 mmol). The crude product was washed with ethanol, and the title compound was collected by filtration as a white solid. An analytically pure sample was obtained from recrystallization in THF at −30 °C (1.04 g, 65%); mp 132−134 °C. ^{1}H NMR ($CDCl_3$, Me_4Si, 270 MHz) δ_H 7.67 (2H, d, $^{3}J_{HH}$ = 6.6 Hz, $^{3}J_{HSn}$ = 58/56 Hz, Acenap 4,7-H), 7.24 (2H, d, $^{3}J_{HH}$ = 6.6 Hz, Acenap 3,8-H), 3.34 (4H, s, Acenap 2 × CH_2), 0.34 (18H, s, $^{3}J_{HSn}$ = 53/51 Hz, 6 × SnCH_3); ^{13}C{^{1}H} NMR ($CDCl_3$, Me_4Si, 76 MHz) δ_C 148.1 (q), 143.7 (q), 139.8 (q), 139.3 (s, $^{3}J_{CSn}$ = 32 Hz, Acenap 4,7-C), 138.6 (q), 119.0 (s, $^{4}J_{CSn}$ = 53 Hz, Acenap 3,8-C), 29.9 (s, Acenap 2 × CH_2), 18.5 (q), −4.5 (s, $^{2}J_{CSn}$ = 347/331 Hz, 6 × $SnCH_3$); ^{119}Sn{^{1}H} NMR ($CDCl_3$, Me_4Sn, 101 MHz) δ_{Sn} −24.3 (s, J_{SnSn} = 37 Hz); MS (ES$^+$): *m/z* (%) 134.93 (100) [SnMe], 164.97 (28) [$SnMe_3$], 197.00 (24) [$SnMe_3OMe$], 303.02 (5) [$C_{12}H_8SnMe_3$], 349.02 (7) [$M^+ - SnMe_3$ + OMe]; Anal. Calcd for $C_{18}H_{26}Sn_2$: C, 45.06; H, 5.46. Found: C, 45.18; H, 5.45.

[Acenap$_2$(SnMe$_2$)$_2$] (3). Experimental details were the same as for compound **1** but with [Acenap(Br)$_2$] (1.12 g, 3.60 mmol), TMEDA (1.6 mL, 9.74 mmol), 2.5 M solution of *n*-butyllithium in hexane (3.2 mL, 7.93 mmol) and Me_2SnCl_2 (1.58 g, 7.19 mmol). The crude product was washed with ethanol, and the title compound was collected by filtration as a white solid. An analytically pure sample was obtained by recrystallization from chloroform (0.28 g, 60%); mp 215−217 °C (decomp); ^{1}H NMR ($CDCl_3$, Me_4Si, 270 MHz) δ_H 7.75 (4H, d, $^{3}J_{HH}$ = 6.9 Hz, $^{3}J_{HSn}$ = 59 Hz, 2 × Acenap 4,7-H), 7.30 (4H, d, $^{3}J_{HH}$ = 6.9 Hz, $^{4}J_{HSn}$ = 83 Hz, 2 × Acenap 3,8-H), 3.37 (8H, s, 2 × Acenap 2 × CH_2), 0.61 (12H, s, $^{2}J_{HSn}$ = 52 Hz, 4 × SnCH_3); ^{13}C{^{1}H} NMR ($CDCl_3$, Me_4Si, 76 MHz) δ_C 148.3 (q), 142.7 (q), 139.7 (q), 139.6 (q), 138.4 (s, $^{3}J_{CSn}$ = 38 Hz, Acenap 4,7-C), 119.4 (s, $^{4}J_{CSn}$ = 57 Hz, Acenap 3,8-C), 30.0 (s, Acenap 4xCH_2), −3.1 (s, $^{2}J_{CSn}$ = 366 Hz, 4 × $SnCH_3$); ^{119}Sn{^{1}H} NMR ($CDCl_3$, Me_4Sn, 101 MHz) δ_{Sn} −60.3 (s, J_{SnSn} = 65 Hz); MS (ES$^+$): *m/z* (%) 602.96 (90) [M^+], 624.98 (100) [M + Na]; Anal. Calcd for $C_{28}H_{28}Sn_2$: C, 55.87; H, 4.69. Found: C, 55.95; H, 4.89.

[Acenap(PPh$_2$)(P^{i}Pr$_2$)] (4). To a cooled (−78 °C), rapidly stirring solution of [Acenap(Br)(P^{i}Pr$_2$)] (4.00 g, 11.5 mmol) in THF (60 mL) was added dropwise (over 1 h) a solution of *n*-butyllithium (2.5 M) in hexane (4.6 mL, 11.5 mmol). The solution was left to stir at this temperature for a further 2 h. To this, a solution of chlorodiphenylphosphine (2.52 g, 2.0 mL, 11.5 mmol) in THF (8 mL) was added dropwise over a 1 h period. The solution was left to warm to room temperature overnight. The volatiles were removed *in vacuo* and replaced with diethyl ether (100 mL) and washed with degassed water (20 mL). The yellow organic layer was separated and dried over magnesium sulfate. Volatiles were again removed *in vacuo* to give a yellow solid that was dried *in vacuo* for 2 h (4.50 g, 87%). ^{1}H NMR ($CDCl_3$, Me_4Si, 500 MHz) δ_H 7.83 (1H, dd, $^{3}J_{HH}$ = 7.2 Hz, $^{3}J_{HP}$ = 2.7 Hz, Acenap 7-H), 7.50−7.43 (4H, m, P*Ph-o*), 7.45−7.42 (1H, m, Acenap 8-H), 7.42−7.36 (6H, m, P*Ph-m,p*), 7.34 (1H, dd, $^{3}J_{HH}$ = 7.3 Hz, $^{3}J_{HP}$ = 4.3 Hz, Acenap 4-H), 7.25 (1H, d, $^{3}J_{HH}$ = 7.3 Hz, Acenap 3-H), 3.53−3.41 (4H, m, Acenap 2 × CH_2), 2.30 (2H, m (∼t sept), $^{2}J_{HP}$ = 14.0 Hz, $^{3}J_{HH}$ = 6.9 Hz, $^{6}J_{HP}$ = 2.2 Hz, PC*H* 13-H), 1.26 (6H, dd, $^{3}J_{HP}$ = 13.0 Hz, $^{3}J_{HH}$ = 6.9 Hz, 2 × CH_3 14-H), 0.87 (6H, dd, $^{3}J_{HP}$ = 11.4 Hz, $^{3}J_{HH}$ = 6.9 Hz, 2 × CH_3, 14-H); ^{13}C{^{1}H} NMR ($CDCl_3$, Me_4Si, 126 MHz) δ_C 148.4(q), 148.3 (q), 141.2 (dd, $^{1}J_{CP}$ = 27.3 Hz, $^{5}J_{CP}$ = 4.2 Hz, 15-qC), 140.0 (dd, $^{3}J_{CP}$ = 6.0 Hz, $^{3}J_{CP}$ = 1.8 Hz, Acenap 1a-qC), 139.6 (dd, $^{2}J_{CP}$ = 26.3 Hz, $^{2}J_{CP}$ = 20.0 Hz, Acenap 5a-qC), 138.0 (s, Acenap 4-C), 135.0 (s, Acenap 7-C), 134.6 (dd, $^{2}J_{CP}$ = 17.8 Hz, $^{6}J_{CP}$ = 3.1 Hz, P*Ph-o*), 131.8 (dd, $^{1}J_{CP}$ = 26.4 Hz, $^{3}J_{CP}$ = 6.0 Hz, Acenap 5-qC), 131.2 (dd, $^{1}J_{CP}$ = 27.0 Hz, $^{3}J_{CP}$ = 8.9 Hz, Acenap 6-qC), 128.3 (d, $^{3}J_{CP}$ = 6.1 Hz, P*Ph-m*), 127.8 (s, P*Ph-p*), 119.6 (s, Acenap 3-C), 119.5 (s, Acenap 8-C), 30.3 (s, Acenap CH_2), 30.0 (s, Acenap CH_2), 26.5 (dd, $^{1}J_{CP}$ = 17.2 Hz, $^{5}J_{CP}$ = 6.2 Hz, PCH 13-C), 20.2 (dd, $^{2}J_{CP}$ = 18.0 Hz, $^{6}J_{CP}$ = 3.3 Hz, 2 × CH_3 14-C), 20.0 (dd, $^{2}J_{CP}$ = 11.7 Hz, $^{6}J_{CP}$ = 2.6 Hz, 2 × CH_3 14-C); ^{31}P NMR ($CDCl_3$, H_3PO_4, 203 MHz) AB spin system: δ_P −11.3 (dd of sept, $^{4}J_{PP}$ = 180.0 Hz, $^{2}J_{PH}$ = 24.5 Hz, $^{3}J_{PH}$ = 11.8 Hz, P_A), −12.8 (d, $^{4}J_{PP}$ = 180.0 Hz, P_B); ^{31}P{^{1}H} NMR ($CDCl_3$, H_3PO_4, 203 MHz) AB spin system: δ_P −11.3 (d, $^{4}J_{PP}$ = 180.0 Hz, P_A), −12.8 (d, $^{4}J_{PP}$ = 180.0 Hz, P_B); HRMS (ES +): *m/z*: Calcd for (M + H) $C_{30}H_{33}P_2$: 455.2057, found: 455.2048; Anal. Calcd for $C_{30}H_{32}P_2$: C, 79.28; H, 7.10. Found: C, 79.18; H, 7.04.

[Acenap(S═PPh$_2$)(S═P^{i}Pr$_2$)] (4-S). Elemental sulfur (0.14 g, 4.40 mmol) and [Acenap(PPh$_2$)(P^{i}Pr$_2$)] (**4**) (1.00 g, 2.20 mmol) in dry toluene (50 mL) were heated under reflux for 3 h. After cooling to room temperature, the volatiles were removed *in vacuo* to give the title compound as a pale-yellow powder (0.88 g, 77%); mp 203−205 °C. Crystals suitable for X-ray diffraction were grown from vapor diffusion of hexane into a saturated solution of the compound in dichloromethane. ^{1}H NMR ($CDCl_3$, Me_4Si, 500 MHz) δ_H 8.90 (1H, dd, $^{3}J_{HP}$ = 16.9 Hz, $^{3}J_{HH}$ = 7.3 Hz, Acenap 7-H), 7.52 (1H, dd, $^{3}J_{HP}$ = 19.6 Hz, $^{3}J_{HH}$ = 7.3 Hz, Acenap 4-H), 7.50 (1H, d, $^{3}J_{HH}$ = 7.3 Hz, Acenap 8-H), 7.46−7.39 (4H, m, P*Ph-o*), 7.39−7.34 (2H, dt, $^{3}J_{HH}$ = 7.2 Hz, $^{4}J_{HH}$ = 1.5 Hz, P*Ph-p*), 7.31−7.27 (4H, m, P*Ph-m*), 7.15 (1H, d, $^{3}J_{HH}$ = 7.3 Hz, 3-H), 4.03−3.94 (2H, m ∼sept, $^{3}J_{HH}$ = 6.6 Hz, PC*H* H-13), 3.51−3.42 (4H, m, Acenap 2 × CH_2), 1.29 (6H, dd, $^{3}J_{HP}$ = 17.6 Hz, $^{3}J_{HH}$ = 6.5 Hz, 2xCH_3 14-H), 0.19 (6H, dd, $^{3}J_{HP}$ = 18.5 Hz, $^{3}J_{HH}$ = 6.9 Hz, 2 × CH_3 14-H); ^{13}C{^{1}H} NMR ($CDCl_3$, Me_4Si, 126 MHz) δ_C 153.1 (q), 151.5 (q), 144.9 (d, $^{2}J_{CP}$ = 10.5 Hz, Acenap 7-C), 142.4 (d, $^{2}J_{CP}$ = 13.7 Hz, Acenap 4-C), 139.1 (dd, $^{3}J_{CP}$ = 10.6 Hz, $^{3}J_{CP}$ = 8.7 Hz, Acenap 1a-qC), 135.1 (d, $^{1}J_{CP}$ = 85.7 Hz, 15-qC), 133.7 (dd, ∼t, $^{2}J_{CP}$ = 8.7, $^{2}J_{CP}$ = 8.7 Hz, Acenap 5a-qC), 131.8 (d, $^{2}J_{CP}$ = 10.0 Hz, P*Ph-o*), 131.1 (d, $^{4}J_{CP}$ = 2.9 Hz, P*Ph-p*), 128.5 (d, $^{3}J_{CP}$ = 12.4 Hz, P*Ph-m*), 126.2 (d, $^{1}J_{CP}$ = 59.9 Hz, Acenap 6-qC), 123.2 (d, $^{1}J_{CP}$ = 84.4 Hz, Acenap 5-qC), 120.3 (d, $^{3}J_{CP}$ = 12.4 Hz, Acenap 8-C), 118.5 (d, $^{3}J_{CP}$ = 14.9 Hz, Acenap 3-C), 30.4 (s, Acenap CH_2), 30.0 (s, Acenap CH_2), 29.6 (d, $^{1}J_{CP}$ = 48.0 Hz, PCH 13-C), 17.8 (d, $^{2}J_{CP}$ = 2.1 Hz, 2 × CH_3 14-C), 17.0 (d, $^{2}J_{CP}$ = 2.1 Hz, 2 ×H_3 14-C); ^{31}P NMR ($CDCl_3$, H_3PO_4, 203 MHz) δ_P 82.0 (br s, P_A), 48.8−48.3 (m, P_B); ^{31}P{^{1}H} NMR ($CDCl_3$, H_3PO_4, 203 MHz) δ_P 82.0 (s, P_A), 48.6 (s, P_B); MS (ES+): *m/z* (%) 541.13 (100) [M + Na], 487.19 (20) [M − S + H]; Anal. Calcd for $C_{30}H_{32}P_2S_2$: C, 69.47; H, 6.22. Found: C, 69.31; H, 6.18.

[Acenap(PPh$_2$)(P^{i}Pr$_2$)]PtCl$_2$ (4-Pt). To a suspension of dichloro(1,5-cyclooctadiene)platinum(II) (0.33 g, 0.88 mmol) in dichloromethane (6 mL) was added dropwise a solution of **4** (0.40 g, 0.88 mmol) in dichloromethane (20 mL). The solution was left to stir at room temperature overnight. The volatiles were removed *in vacuo* to give a white powder (0.55 g, 87%); mp >250 °C. ^{1}H NMR ($CDCl_3$, Me_4Si, 500 MHz) δ_H 7.99 (1H, dd, $^{3}J_{HP}$ = 9.8 Hz, $^{3}J_{HH}$ = 7.5 Hz, Acenap 7-H), 7.57 (1H, d, $^{3}J_{HH}$ = 7.5 Hz, Acenap 8-H), 7.51−7.47 (2H, m, P*Ph-o*), 7.46−7.43 (2H, m, P*Ph-o*), 7.43−7.38 (6H, m, P*Ph-m,p*), 7.35 (1H, dd, $^{3}J_{HH}$ = 7.4 Hz, $^{4}J_{HH}$ = 1.2 Hz, Acenap 3-H), 7.20 (1H, dd, $^{3}J_{HP}$ = 13.3 Hz, $^{3}J_{HH}$ = 7.4 Hz, Acenap 4-H), 3.58−3.51 (4H, m, Acenap 2 × CH_2), 3.49−3.37 (2H, m, ∼2*d* sept, $^{2}J_{HP}$ = 18.6 Hz, $^{3}J_{HH}$ = 7.0 Hz, 1 × PC*H* 13-H, and $^{2}J_{HP}$ = 16.5 Hz, $^{3}J_{HH}$ = 5.5 Hz, 1 × PC*H* 13-H), 1.26 (6H, dd, $^{3}J_{HP}$ = 17.9, $^{3}J_{HH}$ = 7.0 Hz, 2 × CH_3 14-H), 0.92 (6H, dd, $^{3}J_{HP}$ = 16.2 Hz, $^{3}J_{HH}$ = 7.0 Hz, 2 × CH_3 14-H); ^{13}C{^{1}H} NMR ($CDCl_3$, Me_4Si, 126 MHz) δ_C 153.4 (q), 153.0 (q), 139.8 (dd (∼t), $^{3}J_{CP}$ = 8.5 Hz, $^{3}J_{CP}$ = 8.5 Hz, Acenap 1a-qC), 139.1 (d, $^{2}J_{CP}$ = 5.8

dx.doi.org/10.1021/ic5014768 | Inorg. Chem. 2014, 53, 8795−8808

Hz, Acenap 4-C), 137.1 (dd, $^2J_{CP}$ = 12.3 Hz, $^2J_{CP}$ = 8.7 Hz, Acenap 5a-qC), 134.4 (d, $^2J_{CP}$ = 2.8 Hz, Acenap 7-C), 134.0 (d, $^2J_{CP}$ = 10.7 Hz, P*Ph-o*), 131.1 (d, $^2J_{CP}$ = 2.4 Hz, P*Ph-o*), 129.8 (d, $^1J_{CP}$ = 69.2 Hz, 15-qC), 128.6 (s, P*Ph-p*), 128.2 (d, $^3J_{CP}$ = 11.9 Hz, P*Ph-m*), 119.8 (d, $^3J_{CP}$ = 10.7 Hz, Acenap 8-C), 119.3 (d, $^3J_{CP}$ = 8.9 Hz, Acenap 3-C), 112.8 (dd, $^1J_{CP}$ = 74.9 Hz, $^3J_{CP}$ = 8.4 Hz, Acenap 5-qC), 110.6 (dd, $^1J_{CP}$ = 50.3 $^3J_{CP}$ = 9.8 Hz, Acenap 6-qC), 30.4 (s, Acenap CH_2), 30.3 (s, Acenap CH_2), 27.9 (d, $^1J_{CP}$ = 36.2 Hz, PC*H* 13-C), 19.1 (s, 2 × CH_3 14-C), 17.7 (s, 2 × CH_3 14-C); ^{31}P NMR ($CDCl_3$, H_3PO_4, 203 MHz) δ_P 13.4 (m, $^1J_{PPt}$ = 3351 Hz, P_A), −2.3 (m, $^1J_{PPt}$ = 3405 Hz, P_B); ^{31}P{^{1}H} NMR ($CDCl_3$, H_3PO_4, 203 MHz) δ_P 13.4 (d, $^1J_{PPt}$ = 3351 Hz, $^2J_{PP}$ = 26.1 Hz, P_A), −2.3 (d, $^1J_{PPt}$ = 3405 Hz, $^2J_{PP}$ = 26.1 Hz, P_B); ^{195S}Pt{^{1}H} NMR (CD_2Cl_2, Na($PtCl_6$), 107.0 MHz) δ_{Pt} −4504.1 (dd, $^1J_{PPt}$ = 3407.3 Hz, 3351.9 Hz); MS (ES^-): *m*/*z* (%) 719.32 (100) [M − H]; Anal. Calcd for $C_{30}H_{32}P_2Cl_2Pt$: C, 50.01; H, 4.48. Found: C, 49.92; H, 4.57.

[Acenap(PPh$_2$)(P^{i}Pr$_2$)]Mo(CO)$_4$ (4-Mo). To a suspension of $Mo(CO)_4$(nbd) (0.35 g, 1.1 mmol) in dichloromethane (20 mL) was added dropwise a solution of **4** (0.50 g, 1.1 mmol) in dichloromethane (15 mL). The solution was left to stir at room temperature overnight. The volatiles were removed *in vacuo* to give a pale-brown powder. Analytically pure material was obtained by recrystallization from dichloromethane/hexane at room temperature (0.45 g, 60%); mp 236 °C. ^{1}H NMR ($CDCl_3$, Me_4Si, 500 MHz) δ_H 7.77 (1H, dd, ∼t, $^3J_{HP}$ = 7.8 Hz, $^3J_{HH}$ = 7.8 Hz, Acenap 7-H), 7.43−7.35 (11H, m, Acenap 8-H, P*Ph-o,m,p*), 7.29 (1H, dd, $^3J_{HP}$ = 11.0 Hz, $^3J_{HH}$ = 7.3 Hz, Acenap 4-H), 7.21 (1H, d, $^3J_{HH}$ = 7.3 Hz, Acenap 3-H), 3.50−3.42 (4H, m, Acenap 2 × C*H*$_2$), 2.25−2.17 (2H, m, ∼d sept, $^3J_{HH}$ = 7.1 Hz, PC*H* 13-H), 0.98 (6H, dd, $^3J_{HP}$ = 14.9 Hz, $^3J_{HH}$ = 6.9 Hz, 2 × C*H*$_3$ 14-H), 0.92 (6H, dd, $^3J_{HP}$ = 15.8 Hz, $^3J_{HH}$ = 7.0 Hz, 2 × C*H*$_3$ 14-H); ^{13}C{^{1}H} NMR ($CDCl_3$, Me_4Si, 126 MHz) δ_C 218.2 (dd, $^2J_{CP}$ = 23.3 Hz, $^2J_{CP}$ = 8.9 Hz, CO 19-qC), 215.0 (dd, $^2J_{CP}$ = 23.4 Hz, $^2J_{CP}$ = 9.9 Hz, CO 21-qC), 211.4 (dd, ∼t, $^2J_{CP}$ = 9.0 Hz, $^2J_{CP}$ = 9.0 Hz, CO 20-qC), 151.7 (q), 150.3 (q), 141.0 (dd, ∼t, $^2J_{CP}$ = 7.8 Hz, $^3J_{CP}$ = 7.7 Hz, Acenap 1a-qC), 139.5 (s, Acenap 4-C), 138.8 (dd, $^1J_{CP}$ = 33.7 Hz, $^5J_{CP}$ = 2.9 Hz, 15-qC), 138.0 (dd, $^2J_{CP}$ = 18.1 Hz, $^2J_{CP}$ = 13.0 Hz, Acenap 5a-qC), 132.7 (s, P*Ph-o*), 132.6 (s, Acenap 7-C), 128.1 (s, P*Ph-p*), 128.0 (s, P*Ph-m*), 125.1 (dd, $^1J_{CP}$ = 22.5 Hz, $^3J_{CP}$ = 3.0 Hz, Acenap 6-qC), 123.8 (dd, $^1J_{CP}$ = 29.8 Hz, $^3J_{CP}$ = 2.1 Hz, Acenap 5-qC), 119.2 (d, $^3J_{CP}$ = 6.3 Hz, Acenap 3-C), 118.8 (d, $^3J_{CP}$ = 5.3 Hz, Acenap 8-C), 31.0 (s, Acenap CH_2), 30.0 (s, Acenap CH_2), 28.7 (dd, $^1J_{CP}$ = 16.2 Hz, $^5J_{CP}$ = 3.3 Hz, PC*H* 13-C), 18.6 (d, $^2J_{CP}$ = 5.1 Hz, 2 × *C*H$_3$ 14-C), 17.7 (d, $^2J_{CP}$ = 4.7 Hz, 2 × CH$_3$ 14-C); ^{31}P NMR ($CDCl_3$, H_3PO_4, 203 MHz) δ_P 43.7−42.6 (m, P_A), 34.7−34.0 (m, P_B); ^{31}P{^{1}H} NMR ($CDCl_3$, H_3PO_4, 203 MHz) δ_P 43.1 (d, $^2J_{PP}$ = 33.5 Hz, P_A), 34.5 (d, $^2J_{PP}$ = 33.5 Hz, P_B). Anal. Calcd for $C_{34}H_{32}P_2MoO_4$: C, 61.64; H, 4.87. Found: C, 60.66; H, 6.49.

[Acenap(PPh^{i}Pr)(P^{i}Pr$_2$)] (5). To a cooled (−78 °C), rapidly stirring solution of [Acenap(Br)(P^{i}PrPh)] **7** (4.00 g, 11.5 mmol) in THF (60 mL) was added dropwise a solution of *n*-butyllithium (2.5 M) in hexane (4.6 mL, 11.5 mmol) over 1 h. The solution was left to stir at −20 °C for a further hour before being recooled to −78 °C. To this a solution of chlorodiisopropylphosphine (1.75 g, 1.83 mL, 11.5 mmol) in THF (8 mL) was added dropwise over a 1 h period. The solution was left to warm to room temperature overnight. The volatiles were removed *in vacuo* and replaced with diethyl ether (100 mL) and washed with degassed water (20 mL). The yellow organic layer was separated and dried over magnesium sulfate. Volatiles were again removed *in vacuo* to give a yellow oil that was dried *in vacuo* for 2 h. Solid material was obtained by storing the oil at −35 °C (3.77 g, 78%). ^{1}H NMR ($CDCl_3$, Me_4Si, 500 MHz) δ_H 7.93 (1H, dd, $^3J_{HH}$ = 7.2 Hz, $^3J_{HP}$ = 3.3 Hz, Acenap 7-H), 7.15 (1H, dd, $^3J_{HH}$ = 7.1 Hz, $^3J_{HP}$ = 2.9 Hz, Acenap 4-H), 7.71−7.67 (2H, m, P*Ph-o*), 7.42 (1H, d, $^3J_{HH}$ = 7.2 Hz, Acenap 8-H), 7.37 (1H, d, $^3J_{HH}$ = 7.1 Hz, Acenap 3-H), 7.35−7.31 (2H, m, P*Ph-m*), 7.30−7.27 (1H, m, P*Ph-p*), 4.96 (4H, s, Acenap 2 × C*H*$_2$), 2.67−2.59 (1H, m ∼ddh, $^3J_{HH}$ = 7.0 Hz, $^2J_{HP}$ = 4.1 Hz, $^6J_{HP}$ = 2.8 Hz, PC*H* 16-H), 2.44−2.35 (1H, m, PC*H* 19-H), 2.26−2.18 (1H, m ∼ddh, $^2J_{HP}$ = 13.9 Hz, $^3J_{HH}$ = 7.0 Hz, $^6J_{HP}$ = 2.8 Hz, PC*H* 13-H), 1.38 (3H, dd, $^3J_{HP}$ = 11.7 Hz, $^3J_{HH}$ = 7.1 Hz, C*H*$_3$ 20-H), 1.29 (dd, $^3J_{HP}$ = 12.0 Hz, $^3J_{HH}$ = 7.1 Hz, C*H*$_3$ 21-H), 1.24 (3H, dd, $^3J_{HP}$ = 14.6 Hz, $^3J_{HH}$ = 6.8 Hz, C*H*$_3$ 17-H), 1.23 (3H, dd, $^3J_{HP}$ = 14.4 Hz, $^3J_{HH}$ = 7.1 Hz, C*H*$_3$ 18-H), 1.18 (3H, dd, $^3J_{HP}$ = 13.5 Hz, $^3J_{HH}$ = 6.8 Hz, C*H*$_3$ 15-H), 0.58 (3H, dd, $^3J_{HP}$ = 13.3 Hz, $^3J_{HH}$ = 7.0 Hz, C*H*$_3$ 14-H); ^{13}C{^{1}H} NMR ($CDCl_3$, Me_4Si, 126 MHz) δ_C 148.1 (q), 148.0 (q), 141.4 (dd, $^1J_{CP}$ = 13.1 Hz, $^5J_{CP}$ = 6.7 Hz, 22-qC), 140.2 (d, $^2J_{CP}$ = 21.2 Hz, Acenap 5a-qC), 140.0 (dd, $^3J_{CP}$ = 14.3 Hz, $^3J_{CP}$ = 7.4 Hz, Acenap 1a-qC), 135.1 (s, Acenap 7-C), 134.5 (s, Acenap 4-C), 134.2 (dd, $^2J_{CP}$ = 15.3 Hz, $^6J_{CP}$ = 2.9 Hz, P*Ph-o*), 131.8 (dd, $^1J_{CP}$ = 29.1 Hz, $^3J_{CP}$ = 6.4 Hz, Acenap 5-qC), 131.4 (dd, $^1J_{CP}$ = 28.1 Hz, $^3J_{CP}$ = 5.1 Hz, Acenap 6-qC), 127.6 (d, $^3J_{CP}$ = 6.7 Hz, P*Ph-m*), 127.3 (s, P*Ph-p*), 119.3 (s, Acenap 8-C), 119.2 (s, Acenap 3-C), 30.1 (s, Acenap CH_2), 30.0 (s, Acenap CH_2), 27.7 (dd ∼t, $^1J_{CP}$ = 18.3 Hz, PC*H* 16-C), 26.9 (dd, $^1J_{CP}$ = 17.1 Hz, $^5J_{CP}$ = 5.8 Hz, PC*H* 19-C), 25.7 (dd, $^1J_{CP}$ = 20.8 Hz, $^5J_{CP}$ = 14.6 Hz, PC*H* 13-C), 20.8 (dd, $^2J_{CP}$ = 6.4 Hz, $^6J_{CP}$ = 2.6 Hz, CH_3 21-C), 20.7 (s, CH_3 18-C), 20.6 (d, $^2J_{CP}$ = 18.5 Hz, C*H*$_3$ 17-C), 20.2 (d, $^2J_{CP}$ = 16.1 Hz, C*H*$_3$ 14-C), 20.0 (d, $^2J_{CP}$ = 14.8 Hz, C*H*$_3$ 15-C), 19.6 (dd, $^2J_{CP}$ = 13.1 Hz, $^6J_{CP}$ = 2.7 Hz, CH_3 20-C); ^{31}P NMR ($CDCl_3$, H_3PO_4, 203 MHz) AB spin system: δ_P −9.7 (dd of sept, $^4J_{PP}$ = 160.3 Hz, $^2J_{PH}$ = 25.4 Hz, $^3J_{PH}$ = 12.8 Hz, P_A), −13.4 (br d, $^4J_{PP}$ = 160.3 Hz, P_B); ^{31}P{^{1}H} NMR ($CDCl_3$, H_3PO_4, 203 MHz) AB spin system: δ_P −9.7 (d, $^4J_{PP}$ = 160.3 Hz, P_A), −13.4 (d, $^4J_{PP}$ = 160.3 Hz, P_B); MS (ES^+): *m*/*z* (%): 443.30 (100) [M + Na]; Anal. Calcd for $C_{27}H_{34}P_2$: C, 77.10; H, 8.15. Found: C, 76.92; H, 8.14.

[Acenap(S═PPh$_2$)(S═P^{i}Pr$_2$)] (5-S). Elemental sulfur (0.14 g, 4.40 mmol) and **5** (0.93 g, 2.20 mmol) in dry toluene (50 mL) were heated under reflux for 3 h. After cooling to room temperature, the volatiles were removed *in vacuo* to give the product as a pale-yellow powder. Crystals suitable for X-ray diffraction were grown from vapor diffusion of hexane into a saturated solution of the compound in dichloromethane (0.90 g, 85%); mp 133 °C. ^{1}H NMR ($CDCl_3$, Me_4Si, 500 MHz) δ_H 8.68 (1H, dd, $^3J_{HP}$ = 16.5 Hz, $^3J_{HH}$ = 7.3 Hz, Acenap 7-H), 8.20 (1H, dd, $^3J_{HP}$ = 15.8 Hz, $^3J_{HH}$ = 7.3 Hz, Acenap 4-H), 7.60−7.53 (2H, m, P*Ph-o*), 7.47−7.42 (3H, m, Acenap 3,8-H, P*Ph-p*), 7.40−7.35 (2H, m, P*Ph-m*), 3.95−3.83 (1H, br s, PC*H* 16-H), 3.50−3.39 (1H, m, PC*H* 13-H), 3.45 (4H, s, Acenap 2 × C*H*$_2$), 2.72−2.63 (1H, m, PC*H* 19-H), 1.19 (3H, dd, $^3J_{HP}$ = 17.6 Hz, $^3J_{HH}$ = 6.6 Hz, C*H*$_3$ 17-H), 1.07 (3H, dd, $^3J_{HP}$ = 17.2 Hz, $^3J_{HH}$ = 6.7 Hz, C*H*$_3$ 15-H), 0.84 (3H, dd, $^3J_{HP}$ = 18.7 Hz, $^3J_{HH}$ = 6.8 Hz, C*H*$_3$ 20-H), 0.59 (3H, dd, $^3J_{HP}$ = 18.0 Hz, $^3J_{HH}$ = 6.8 Hz, C*H*$_3$ 21-H), 0.43 (3H, dd $^3J_{HP}$ = 18.0 Hz, $^3J_{HH}$ = 6.8 Hz, C*H*$_3$ 18-H), 0.30 (3H, dd, $^3J_{HP}$ = 18.6 Hz, $^3J_{HH}$ = 6.9 Hz, C*H*$_3$ 14-H); ^{13}C{^{1}H} NMR ($CDCl_3$, Me_4Si, 126 MHz) δ_C 152.6 (q), 150.9 (q), 143.6 (br s, Acenap 7-C), 139.6 (dd ∼t, $^2J_{CP}$ = 9.4 Hz, Acenap 1a-qC), 137.6 (d, $^2J_{CP}$ = 9.4 Hz, Acenap 4-C), 133.6 (dd ∼t, $^2J_{CP}$ = 6.6 Hz, Acenap 5a-qC), 132.4 (d, $^2J_{CP}$ = 9.0 Hz, P*Ph-o*), 131.3 (d, $^4J_{CP}$ = 2.4 Hz, P*Ph-p*), 129.6 (d, $^1J_{CP}$ = 74.8 Hz, 22-qC), 128.1 (d, $^3J_{CP}$ = 11.6 Hz, P*Ph-m*), 126.8 (d, $^1J_{CP}$ = 63.7 Hz, Acenap 6-qC), 121.5 (d, $^1J_{CP}$ = 79.7 Hz, Acenap 5-qC), 120.3 (d, $^3J_{CP}$ = 12.7 Hz, Acenap 3-C), 118.4 (d, $^3J_{CP}$ = 13.6 Hz, Acenap 8-C), 36.4 (d, $^1J_{CP}$ = 58.0 Hz, PC*H* 19-C), 30.3 (s, Acenap CH_2), 30.0 (s, Acenap CH_2), 29.5 (d, $^1J_{CP}$ = 47.3 Hz, PC*H* 13-C), 29.2 (d, $^1J_{CP}$ = 45.7 Hz, PC*H* 16-C), 18.0 (s, CH_3 17-C), 17.6 (s, CH_3 15-C), 17.5 (s, CH_3 18-C), 17.2 (s, CH_3 14-C), 17.0 (s, C*H*$_3$ 21-C), 16.2 (s, CH_3 20-C); ^{31}P NMR ($CDCl_3$, H_3PO_4, 203 MHz) δ_P 79.6 (br s, P_A), 56.8 (br s, P_B); ^{31}P{^{1}H} NMR ($CDCl_3$, H_3PO_4, 203 MHz) δ_P 79.6 (br s, P_A), 56.8 (s, P_B); MS (ES^+): *m*/*z* (%): 507.15 (100) [M + Na]; Anal. Calcd for $C_{27}H_{34}P_2S_2$: C, 66.90; H, 7.08. Found: C, 67.04; H, 7.10.

[Acenap(Br)(P^{i}PrPh)] (7). To a cooled (−78 °C) rapidly stirring solution of 5,6-dibromoacenaphthene (5.0 g, 16.03 mmol) in tetrahydrofuran (60 mL) was added dropwise a solution of *n*-butyllithium (2.5 M) in hexane (6.4 mL, 16.03 mmol) over 1 h, and the mixture was left to stir for a further 2 h at the same temperature. A solution of chloroisopropylphenylphosphine (2.7 mL, 3.0 g, 16.03 mmol) in tetrahydrofuran (8 mL) was then added over 1.5 h. The solution was allowed to warm up to room temperature overnight. The volatiles were removed *in vacuo,* and the solvent was replaced with diethyl ether (70 mL) and washed with degassed water (25 mL). The organic layer was removed and dried over magnesium sulfate and then was filtered; the solvent was removed *in vacuo* to reveal a yellow solid.

dx.doi.org/10.1021/ic5014768 | *Inorg. Chem.* 2014, 53, 8795−8808

Analytically pure crystals were grown from ethanol (2.4 g, 40%); mp 136 °C. ^{1}H NMR ($CDCl_3$, Me_4Si, 500 MHz) δ_H 7.88 (1H, dd, $^{3}J_{HH}$ = 7.3 Hz, $^{3}J_{HP}$ = 3.1 Hz, Acenap 7-H), 7.72 (1H, d, $^{3}J_{HH}$ = 7.4 Hz, Acenap 4-H), 7.60−7.53 (2H, m, P*Ph-o*), 7.38 (1H, d, $^{3}J_{HH}$ = 7.3 Hz, Acenap 8-H), 7.35−7.29 (3H, m, P*Ph-m,p*), 7.06 (1H, d, $^{3}J_{HH}$ = 7.2 Hz, Acenap 3-H), 3.40−3.25 (4H, m, Acenap 2 × C*H*$_2$), 2.48 (1H, d of sept, $^{3}J_{HH}$ = 6.9 Hz, $^{2}J_{HP}$ = 5.2 Hz, PC*H*), 1.24 (3H, dd, $^{3}J_{HP}$ = 15.4 Hz, $^{3}J_{HH}$ = 6.8 Hz, 1 × C*H*$_3$ 14-H), 1.14 (3H, dd, $^{3}J_{HP}$ = 15.6 Hz, $^{3}J_{HH}$ = 6.8 Hz, 1 × C*H*$_3$ 14-H); ^{13}C{^{1}H} NMR ($CDCl_3$, Me_4Si, 126 MHz) δ_C 148.4 (q), 146.8 (q), 141.7 (q), 140.0 (d, $^{1}J_{CP}$ = 16.6 Hz, 15-qC), 135.2 (broad s, Acenap 7-C), 135.0 (s, Acenap 4-C), 133.8 (d, $^{2}J_{CP}$ = 18.3 Hz, P*Ph-o*), 133.6 (q), 129.7 (d, $^{1}J_{CP}$ = 30.4 Hz, Acenap 6-C), 128.2 (s, P*Ph-p*), 128.1 (d, $^{3}J_{CP}$ = 7.0 Hz, P*Ph-m*), 120.5 (s, Acenap 3-C), 120.1 (s, Acenap 8-C), 115.7 (q), 30.2 (s, Acenap CH_2), 29.8 (s, Acenap CH_2), 27.0 (d, $^{1}J_{CP}$ = 14.2 Hz, PCH), 20.4 (d, $^{2}J_{CP}$ = 19.8 Hz, CH_3 14-C), 19.8 (d, $^{2}J_{CP}$ = 22.3 Hz, CH_3 14-C); ^{31}P NMR ($CDCl_3$, H_3PO_4, 203 MHz) δ_P −9.3−−10.3 (m); ^{31}P{^{1}H} NMR ($CDCl_3$, H_3PO_4, 203 MHz) δ_P −9.7 (s); MS (ES$^+$): *m*/*z* (%) 335.16 (75) [M-Br+OMe ($C_{22}H_{24}PO$)], 383.06 (100) [M$^+$], 413.07 (40) [M + OMe]; HRMS (ES$^+$): *m*/*z*: Calcd for $C_{21}H_{21}PBr$: 383.0564, found 383.0553; Calcd for $C_{22}H_{23}POBr$: 413.0669, found 413.0658; Calcd for $C_{22}H_{24}OP$: 335.1565, found 335.1554; Anal. Calcd for $C_{21}H_{20}PBr$: C, 65.81; H, 5.26. Found: C, 65.79; H, 5.34.

CRYSTAL STRUCTURE ANALYSES

The X-ray crystal structure for **1** was determined at −100(1) °C using a Rigaku XtaLAB P100 diffractometer (Mo Kα radiation, confocal optic). Intensities were corrected for Lorentz, polarization, and absorption. Data for **2** were determined at −148(1) °C with the St. Andrews Robotic Diffractometer,[32] a Rigaku ACTOR-SM, and a Saturn 724 CCD area detector with graphite-monochromated Mo Kα radiation (λ =0.71073 Å). Data were corrected for Lorentz, polarization, and absorption. Data for compound **4-Pt** were collected at −148(1) °C with a Rigaku SCXmini CCD area detector with graphite-monochromated Mo Kα radiation (λ = 0.71073 Å). Data were corrected for Lorentz, polarization, and absorption. Data for compounds **3** and **4-Mo** were collected at −148(1) °C, for **4**, **4-S**, and **5-S** at −180(1) °C, and for **7** at −100(1) °C using a Rigaku MM007 high-brilliance RA generator (Mo Kα radiation, confocal optic) and Mercury CCD system. At least a full hemisphere of data was collected using ω scans. Data for all the compounds analyzed were collected and processed using CrystalClear (Rigaku).[33] Structures were solved by direct methods[34] and expanded using Fourier techniques.[35] Non-hydrogen atoms were refined anisotropically. Hydrogen atoms were refined using the riding model. All calculations were performed using the CrystalStructure[36] crystallographic software package except for refinement, which was performed using SHELXL2013.[37] These X-ray data can be obtained free of charge via www.ccdc.cam.ac.uk/conts/retrieving.html or from the Cambridge Crystallographic Data Centre, 12 Union Road, Cambridge CB2 1EZ, UK; fax (+44) 1223-336-033; e-mail: deposit@ccdc.cam.ac.uk.

ASSOCIATED CONTENT

Supporting Information

Additional experimental details (including ^{31}P and ^{195}Pt NMR spectra), crystallographic data and figures. This material is available free of charge via the Internet at http://pubs.acs.org.

AUTHOR INFORMATION

Corresponding Authors

*J.D.W.: Fax: (+44) 1334-463384. E-mail: jdw3@st-and.ac.uk.
*P.K.: E-mail: pk7@st-and.ac.uk.

Notes

The authors declare no competing financial interest.

ACKNOWLEDGMENTS

Elemental analyses were performed by Stephen Boyer at the London Metropolitan University. Mass spectrometry measurements were performed by Caroline Horsburgh at the University of St Andrews Mass Spectrometry Service. The work in this project was supported by the Engineering and Physical Sciences Research Council (EPSRC), EaStCHEM and the University of St Andrews.

REFERENCES

(1) Balasubramaniyan, V. *Chem. Rev.* **1966**, *66*, 567.
(2) Kilian, P.; Knight, F. R.; Woollins, J. D. *Chem.—Eur. J.* **2011**, *17*, 2302.
(3) For example, see: (a) Katz, H. E. *J. Am. Chem. Soc.* **1985**, *107*, 1420. (b) Alder, R. W.; Bowman, P. S.; Steel, W. R. S.; Winterman, D. R. *Chem. Commun.* **1968**, 723. (c) Costa, T.; Schimdbaur, H. *Chem. Ber.* **1982**, *115*, 1374. (d) Karaçar, A.; Freytag, M.; Thönnessen, H.; Omelanczuk, J.; Jones, P. G.; Bartsch, R.; Schmutzler, R. *Heteroat. Chem.* **2001**, *12*, 102. (e) Glass, R. S.; Andruski, S. W.; Broeker, J. L.; Firouzabadi, H.; Steffen, L. K.; Wilson, G. S. *J. Am. Chem. Soc.* **1989**, *111*, 4036. (f) Fuji, T.; Kimura, T.; Furukawa, N. *Tetrahedron Lett.* **1995**, *36*, 1075. (g) Schiemenz, G. P. *Z. Anorg. Allg. Chem.* **2002**, *628*, 2597. (h) Corriu, R. J. P.; Young, J. C. Hypervalent Silicon Compounds. In *Organic Silicon Compounds*; Patai, S., Rappoport, Z., Eds.; Wiley: Chichester, U.K., 1989; Vols. *1* and *2*.
(4) Ray, M. J.; Randall, R. A. M.; Athukorala Arachchige, K. S.; Slawin, A. M. Z.; Bühl, M.; Lebl, T.; Kilian, P. *Inorg. Chem.* **2013**, *52*, 4346.
(5) Somisara, D. M. U. K.; Bühl, M.; Lebl, T.; Richardson, N. V.; Slawin, A. M. Z.; Woollins, J. D.; Kilian, P. *Chem.—Eur. J.* **2011**, *17*, 2666.
(6) Omelańczuk, J.; Karaçar, A.; Freytag, M.; Jones, P. G.; Bartsch, R.; Mikołajczyk, M.; Schmutzler, R. *Inorg. Chim. Acta* **2003**, *350*, 583.
(7) Owsianik, K.; Vendier, L.; Błaszczyk, J.; Sieroń, L. *Tetrahedron* **2013**, *69*, 1628.
(8) Jiang, C.; Blacque, O.; Berke, H. *Chem. Commun.* **2009**, 5518.
(9) (a) Blount, J. F.; Cozzi, F.; Damewood, J. R., Jr.; Iroff, L. D.; Sjöstrand, U.; Mislow, K. *J. Am. Chem. Soc.* **1980**, *102*, 99. (b) Seyferth, D.; Vick, S. C. *J. Organomet. Chem.* **1977**, *141*, 173.
(10) Handal, J.; White, J. G.; Franck, R. W.; Yuh, Y. H.; Allinger, N. L. *J. Am. Chem. Soc.* **1977**, *99*, 3345.
(11) Allen, F. H. *Acta Crystallogr.* **2002**, *B58*, 380.
(12) Bondi, A. *J. Phys. Chem.* **1964**, *68*, 441.
(13) (a) Nakanishi, W.; Hayashi, S.; Toyota, S. *Chem. Commun.* **1996**, 371. (b) Nakanishi, W.; Hayashi, S.; Sakaue, A.; Ono, G.; Kawada, Y. *J. Am. Chem. Soc.* **1998**, *120*, 3635. (c) Nakanishi, W.; Hayashi, S.; Toyota, S. *J. Org. Chem.* **1998**, *63*, 8790. (d) Hayashi, S.; Nakanishi, W. *J. Org. Chem.* **1999**, *64*, 6688. (e) Nakanishi, W.; Hayashi, S.; Uehara, T. *J. Phys. Chem. A* **1999**, *103*, 9906. (f) Nakanishi, W.; Hayashi, S.; Uehara, T. *Eur. J. Org. Chem.* **2001**, 3933. (g) Nakanishi, W.; Hayashi, S. *Phosphorus Sulfur Silicon Relat. Elem.* **2002**, *177*, 1833. (h) Nakanishi, W.; Hayashi, S.; Arai, T. *Chem. Commun.* **2002**, 2416. (i) Hayashi, S.; Nakanishi, W. *J. Org. Chem.* **2002**, *67*, 38. (j) Nakanishi, W.; Hayashi, S.; Itoh, N. *Chem. Commun.* **2003**, 124. (k) Hayashi, S.; Wada, H.; Ueno, T.; Nakanishi, W. *J. Org. Chem.* **2006**, *71*, 5574. (l) Hayashi, S.; Nakanishi, W. *Bull. Chem. Soc. Jpn.* **2008**, *81*, 1605.
(14) Panda, A.; Mugesh, G.; Singh, H. B.; Butcher, R. J. *Organometallics* **1999**, *18*, 1986.
(15) (a) Beckmann, J.; Bolsinger, J.; Duthie, A.; Finke, P. *Dalton Trans.* **2013**, *42*, 12193. (b) Beckmann, J.; Bolsinger, J.; Duthie, A. *Chem.—Eur. J.* **2011**, *17*, 930.
(16) (a) Wawrzyniak, P.; Slawin, A. M. Z.; Woollins, J. D.; Kilian, P. *Dalton Trans.* **2010**, *39*, 85. (b) Wawrzyniak, P.; Fuller, A. L.; Slawin, A. M. Z.; Kilian, P. *Inorg. Chem.* **2009**, *48*, 2500. (c) Surgenor, B. A.;

Bühl, M.; Slawin, A. M. Z.; Woollins, J. D.; Kilian, P. *Angew. Chem., Int. Ed.* **2012**, *51*, 10150.
(17) Aschenbach, L. K.; Knight, F. R.; Randall, R. A. M.; Cordes, D. B.; Baggott, A.; Bühl, M.; Slawin, A. M. Z.; Woollins, J. D. *Dalton Trans.* **2012**, *41*, 3141.
(18) Athukorala Arachchige, K. S.; Sanz Camacho, P.; Ray, M. J.; Chalmers, B. A.; Knight, F. R.; Ashbrook, S. E.; Bühl, M.; Kilian, P.; Slawin, A. M. Z.; Woollins, J. D. *Organometallics* **2014**, *33*, 2424.
(19) (a) Kim, Y.; Zhao, H.; Gabbaï, F. P. *Angew. Chem., Int. Ed.* **2009**, *48*, 4957. (b) Zhao, H.; Gabbaï, F. P. *Nat. Chem.* **2010**, *2*, 984.
(20) For example: (a) Gabbaï, F. P.; Schier, A.; Riede, J.; Sladek, A.; Görlitzer, H. W. *Inorg. Chem.* **1997**, *36*, 5694. (b) Lin, T.-P.; Nelson, R. C.; Wu, T.; Miller, J. T.; Gabbaï, F. P. *Chem. Sci.* **2012**, *3*, 1128. (c) Hoefelmeyer, J. D.; Gabbaï, F. P. *Chem. Commun.* **2003**, 712. (d) Tschinkl, M.; Hoefelmeyer, J. D.; Cocker, T. M.; Backman, R. E.; Gabbaï, F. P. *Organometallics* **2000**, *19*, 1826. (e) Lin, T.-P.; Wade, C. R.; Pérez, L. M.; Gabbaï, F. P. *Angew. Chem., Int. Ed.* **2010**, *49*, 6357. (f) Ohshita, J.; Matsushige, K.; Kunai, A. *Organometallics* **2000**, *19*, 5582.
(21) (a) Meinwald, J.; Knapp, S.; Tatsuoka, T. *Tetrahedron Lett.* **1977**, *26*, 2247. (b) Tinga, M. A. G. M.; Buisman, G. J. H.; Schat, G.; Akkerman, O. S.; Bickelhaupt, F.; Smeets, W. J. J.; Spek, A. L. *J. Organomet. Chem.* **1994**, *484*, 137.
(22) Beckmann, J.; Hupf, E.; Lork, E. *Main Group Met. Chem.* **2013**, *36*, 145.
(23) Panisch, R.; Bolte, M.; Muller, T. *J. Am. Chem. Soc.* **2006**, *128*, 9676.
(24) Slawin, A. M. Z.; Williams, D. J.; Wood, P. T.; Woollins, J. D. *Chem. Commun.* **1987**, 1741.
(25) Kilian, P.; Knight, F. R.; Woollins, J. D. *Coord. Chem. Rev.* **2011**, *255*, 1387.
(26) Karacar, A.; Freytag, M.; Jones, P. G.; Bartsch, R.; Schmutzler, R. *Z. Anorg. Allg. Chem.* **2002**, *628*, 533.
(27) The synthesis of **3** has been previously published: Mitchell, R. H.; Chaudhary, M.; Vaughan Williams, R.; Fyles, R.; Gibson, J.; Ashwood-Smith, M. J.; Fry, A. J. *Can. J. Chem.* **1992**, *70*, 1015.
(28) Farah, D.; Swami, K.; Kuivila, H. G. *J. Organomet. Chem.* **1992**, *429*, 311.
(29) Neudorff, W. D.; Lentz, D.; Anibarro, M.; Schlüter, A. D. *Chem.—Eur. J.* **2003**, *9*, 2745.
(30) Nagy, P.; Szabó, D.; Kapovits, I.; Kucsman, Á.; Argay, G.; Kálmán, A. *J. Mol. Struct. (THEOCHEM)* **2002**, *606*, 61.
(31) Hazell, A. C.; Hazell, R. G.; Norskov-Lauritsen, L.; Briant, C. E.; Jones, D. W. *Acta Crystallogr., Sect. C* **1986**, *42*, 690−693.
(32) Fuller, A. L.; Scott-Hayward, L. A. S.; Li, Y.; Bühl, M.; Slawin, A. M. Z.; Woollins, J. D. *J. Am. Chem. Soc.* **2010**, *132*, 5799.
(33) CrystalClear: Rigaku Corporation, 1999. CrystalClear Software User's Guide, Molecular Structure Corporation, (c) 2000 Pflugrath, J. W. *Acta Crystallogr.* **1999**, *D55*, 1718.
(34) Burla, M. C.; Caliandro, R.; Camalli, M.; Carrozzini, B.; Cascarano, G. L.; De Caro, L.; Giacovazzo, C.; Polidori, G.; Spagna, R. *SIR2004*; 2005.
(35) DIRDIF99: Beurskens, P. T.; Admiraal, G.; Beurskens, G.; Bosman, W. P.; de Gelder, R.; Israel, R.; Smits, J. M. M. . *The DIRDIF-99 program system, Technical Report of the Crystallography Laboratory*; University of Nijmegen: The Netherlands, 1999.
(36) *CrystalStructure 4.1: Crystal Structure Analysis Package*; Rigaku Corporation: Tokyo, Japan, 2000−2014
(37) Sheldrick, G. M. *SHELX2013*; University of Gottingen: Germany, 2013.